CRUISE REPORT

SHIP UTIL[illegible]ON DATA

UNOLS Rev.

SHIP NAME: CONRAD	OPERATING INST.: LDGO	PARTICIPATING PERSONNEL
CRUISE (LEG) NO.: 2707	DATES: 8/3/86 - 8/24/86	
AREA OF OPERATIONS: Central Indian Ocean.	PORT CALLS: PLACE: Colombo; Perth — DATES: 8/3/86; 8/24/86	
DAYS AT SEA: 21 ✓ — DAYS IN PORT: 6 ✓		

CODE	NAME	TITLE	AFFILIATION
1.	JOHN G. SCLATER	PROF.	UTIG
2.	ROGER SCRUTTON	PROF	Univ Edinburgh, UK
3.	see xerox copy of Jeff Weissel.		
4.			

Use Reverse If Additional Space Required.

WAS RESEARCH CONDUCTED IN FOREIGN WATERS? _____ COUNTRY: _____

PRIMARY PROJECTS (those which govern the principal operations, area and movements of the ship)

PROJECT TITLE AND PRINCIPAL INVESTIGATOR	SPONSORING ACTIVITY	GRANT OR CONTRACT NUMBER	PARTICIPATING PERSONNEL (AS CODED ABOVE)
INTRAPLATE DEFORMATION IN THE CENTRAL INDIAN OCEAN. JEFF WEISSEL	NSF	?	1 - 10
DISCIPLINE: MG&G			

ANCILLARY PROJECTS (which are accomplished on a not-to-interfere basis and contribute to the overall effectiveness of the cruise)

PROJECT TITLE AND PRINCIPAL INVESTIGATOR	SPONSORING ACTIVITY	GRANT OR CONTRACT NUMBER	PARTICIPATING PERSONNEL (AS CODED ABOVE)
A PROPOSAL FOR MCS DRILLING SITE SURVEYS IN THE INDIAN OCEAN. JOHN G. SCLATER	NSF	?	1 - 10

SIGNATURE: John G. Sclater DATE: _____

1 /CHIEF SCIENTIST

TOTAL SCIENTISTS 4 TOTAL TECHNICIANS 8

TOTAL GRAD STUDENTS 4 TOTAL STUDENTS/OBSERVERS 0

ATTACH PAGE SIZE CRUISE TRACK

COST ALLOCATION DATA

DAYS CHARGED	AGENCY OR ACTIVITY CHARGED	GRANT OR CONTRACT NO.
27	NSF	OCE-83-16163 Columbia 5-24982

SIGNATURE

...gust 15, 1986

R/V ROBERT D. CONRAD
CREW LIST
27-07

DEPARTED: Colombo, Sri Lanka — 31 July 1986
ETA: Perth, Australia — 25 August 1986

1.	Peterlin, John G.	Master
2.	O'Loughlin, James E.	Ch. Mate
3.	Mello, Louis J.	2nd Mate
4.	Collins, Edmund M.	3rd Mate
5.	Heinz, Blaine	Bosun
6.	Bagwell, Samuel	A.B.
7.	Nolan, Timothy J.	A.B.
8.	Zeigler, Stanley P	A.B.
9.	Barros, Larry W.	O.S.
10.	Olander, Hans P.	O.S.
11.	Phillips, Donald E.	Chief Engr.
12.	Smith, John E.	2nd A/E
13.	Mathews, Richard	3rd A/E
14.	Tucke, Matthew S.	3rd A/E
15.	Brow, Robert F.	Oiler
16.	Martin, Peter J.	Oiler
17.	Uribe, Guillermo F.	Oiler
18.	Amarasinghe, A.	Wiper
19.	Dakers, Hugh B.	Steward
20.	Tuiqilai, V.	Messman
21.	Bahl, Lee B.	Messman
22.	Moqo, Luke	Messman

SCIENTIFIC CREW

23.	Smith, James A.	Science Officer
24.	Blauner, Lloyd	Technician
25.	DiBernardo, John	Technician
26.	Iltzsche, Martin W.	Technician
27.	Monakhov, Leonid T.	Technician
28.	Qali, Ropate	Air Gun Tech.
29.	Robinson, Frank	Science Tech.
30.	VanSteveninick, William	Technician

SCIENTISTS

31.	Sclater, John G.	Chief Scientist
32.	Cowie, Patience A.	Scientist
33.	Hobart, Michael A.	Scientist
34.	Joffe, Samuel W.	Scientist
35.	Keyes, Caroline M.	Scientist
36.	Kuo, Ban-Yuan	Scientist
37.	Savdra, Jiri	Scientist
38.	Scrutton, Roger A.	Scientist
39.	Zuber, Maria T.	Scientist

CRUISE REPORT RC27-07
COLOMBO - PERTH

3 August - 25 August, 1986

Participating Personnel
J. G. Sclater, Chief Scientist
R. A. Scrutton, Scientist
M. A. Hobart, Scientist
J. A. Smith, Science Officer
W. Van Steveninck, Technician
P. A. Cowie, Watchstander
M. T. Zuber, Watchstander
S. W. Joffe, Watchstander
B.-Y. Kuo, Watchstander
J. Savrda, Watchstander
L. Monakhov, Watchstander
C. M. Keyes, Technician
F. Robinson, Technician
R. Qali Maiwiriwiri, Technician
M. Iltzsche, Engineer
J. DiBernardo, Technician
L. Blauner, Technician

Introduction
Cruise RC27-07 of R/V ROBERT D. CONRAD left Colombo, Sri Lanka at 1200 (local) 03 August and reached Fremantle, the port of Perth Western Australia on 0800 (local) 25 August, 1986. The scientific objectives included
a) to obtain further heat flow data to complete the investigation of the relationships among high heat flow, intraplate compression, and the upward flow of fluids in the Central Indian Ocean basin begun on RC27-06, and
b) to conduct a site survey on the Ninetyeast Ridge at 17.5°S in preparation for ODP drilling there.

The reports for these two science objectives are attached as PART 1 (Heat Flow Results) by M. Hobart and J. Sclater, and PART 2 (Ninetyeast Ridge Site Survey) by J. Sclater and J. Savrda.

The track for RC27-07 is shown in Fig. 1.

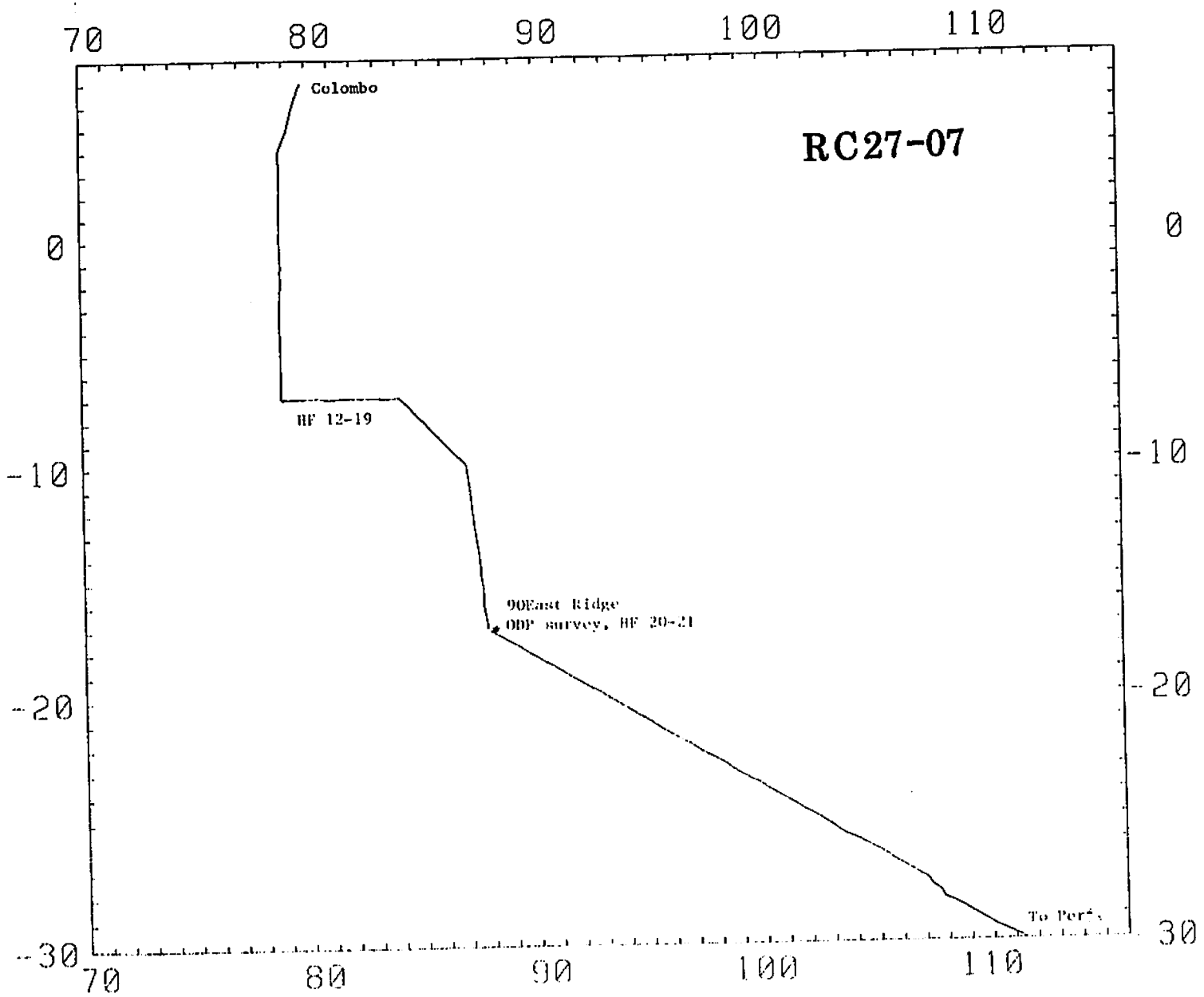
70
80
90
100
110
RC27-07
Colombo
0
-10
-20
-30
BF 12-19
90East Ridge
ODP survey, BF 20-21
To Perth
30

Figure 1

PART 1

REPORT ON HEAT FLOW DATA FROM 7 S

IN THE REGION OF INTRAPLATE DEFORMATION

IN THE CENTRAL INDIAN BASIN

TAKEN ON RC2707

BY

MIKE HOBART

AND

JOHN SCLATER

INTRODUCTION

Deformation of oceanic lithosphere under horizontal compression is more clearly developed in the Central Indian Ocean Basin south of India than in any other part of the ocean. It is noteworthy that the deformation is intraplate as the region affected is remote from the generally accepted boundaries of the Indo-Australian plate (Figure 1).

Heat flow in the region affected by the deformation is highly unusual and may be related to the deformation either as a cause or as a consequence. Abnormally high heat flow values are distributed widely over the Central Indian Ocean Basin(Anderson et al.,1977; Weissel et al.,1980; Geller et al.,1983). Many of the measured temperature-depth profiles are non-linear,suggesting an upward flow of water through the sediments(Geller et al.,1983). Such fluid flow is unusual in view of the thick,uniform cover of Bengal Fan sediments and the age of the underlying crust(>60 MA). In addition, Stark and Forsyth (1983) have identified large shear wave travel time anomalies with an apparent two-dimensional, sinusoidal pattern of delay times that may be associated with linear convection cells in the upper mantle beneath the Central Indian Basin(Figures 2 and 3). The trend and wavelength of these apparent velocity anomalies in the mantle agree with the NNE-SSW trends of long-wavelength (500-600 km) gravity anomalies derived from SEASAT altimeter data shown in Figure 4.

This cruise leg was the second part of a two-leg study to investigate these phenomena using marine geothermal, OBS seismic, and standard marine geophysical techniques.

In this report we cover possible explanations of the high heat flow, the objectives of the east west line of heat flow stations and the actual observations. In the final section we present a preliminary interpretation of the results.

HYPOTHESES FOR HIGH HEAT FLOW

There are five major hypotheses that have been advanced to explain the high heat flow.

1. The high heat flow is a manifestation of the work required to deform the lithosphere (in the form of viscous dissipation, friction on faults, or plastic deformation) (Weissel et al.,1980).

2. The high values result through unusually intense, small-scale mantle convection oriented a) in the direction of "absolute" plate motion (Stark and Forsyth,1982), or b) E-W, providing buoyancy forces which have initiated the long-wavelength undulatory deformation.

3. The heat flow anomalies represent local, temporary conditions associated with upward fluid flow, released or driven out of the sediments (and/or basement) by compressional deformation - a dewatering phenomenon.

4. The high average heat flow is associated with biased sampling of upwelling limbs of hydrothermal convection cells which have been reactived by cracking and faulting of the crust during deformation(Geller et al.,1983).

5. The high heat flow at the distal end of the Bengal Fan represents the discharge zone of artesian flow through permeable sediments in the fan. Faulting associated with the intraplate deformation has allowed such water to reach the sea floor.

Under hypothesis 1 the high heat flow should increase according to the intensity of deformation as observed in seismic reflection profiles. Under hypothesis 2a, heat flow should show an approximately E-W sinsusoidal variation with a wavelength of about 600 km. Under hypothesis 2b, the variation should be in a N-S direction with high values associated with basement highs and low or normal values associated with basement lows. Under hypotheses 3-5, heatflow variations may occur at shorter spatial scales and may correlate with the observed intensity of deformation.

OBJECTIVES OF HEAT FLOW INVESTIGATION

This leg was intended to examine an east west profile to check hypothesis 2a (above). The detailed heat flow sites also bear on hypotheses 3-5.

Seven sites including an earlier 'pogo' run in the same area (Geller et al.,1983) were occupied along 7 S between 78 55 E and 84 00 E. The E-W heat flow profile was run over a prominent gravity and basement high that, in this area, is covered with a relatively undisturbed layer of distal Bengal Fan and pelagic sediments, the uppermost of which were deposited after most of the intraplate deformation took place. These conditions provided a fairly uniform environment for heat flow measurements along most of the 600 km profile. The profile length was chosen to try to detect the 500-600 km wavelength variation suggested by Stark and Forsyth (1982) to be caused by small scale upper-mantle convection aligned with the plate motion.

The individual penetrations at each station along the east-west profile were placed close to each other (about 1 km) in order to permit detection of any oscillatory patterns in the heat flow that would indicate typical hydrothermal convection systems in older crust(Anderson et al.,1979).

Comparison of the average values at each station permit the investigation of the proposed upper-mantle origin for the heat flow anomalies. The individual penetrations and temperature gradients permit the study of convective flow either in the crust or sediments as an explanation of the anomalies.

OBSERVATIONS

We occupied seven successful detailed heat flow stations along a line between 7 S 78 55 E and 7 S 84 00 E. The individual penetrations at each station were taken in an east west direction. In addition a prior survey had been carried out on the same line but trending north south by Geller et al.(1983).We ran a short set of four penetrations along our line just south of their survey area in order to encorporate their data with ours. Most stations consisted of ten to twelve penetrations of the bottom using the LDGO digital heat flow instrument. At the last station on the line two seperate lowerings from the surface were made.

At all of the stations we ran east west into the prevailing wind and seas to take the measurements. We had considerable problems with the elasticity of the winch wire. As a result the wire was repeatedly caught around either one of the fins of the corer or around one of the thermistor mountings. These problems lead to tilting on a number of the penetrations. Other than this there were no problems with the measurements.

No non-linear temperature profiles indicating advection through the sediments were observed. Three cores were taken equally spaced along the profile at the second, fourth and sixth stations. The thermal conductivity was measured on the sediment recovered in these cores using the method of Von Herzen and Maxwell (1959).

Plots of the conductivities as a function of depth are presented as Figure 5. Note that apart from a small lense of high conductivity, presumably a turbite sand, at the bottom of the last core on the line the conductivities vary very little with depth or between cores. The conductivities are also similar to the southernmost core from the previous leg, RC2706.

A summary of the heat flow results from each station is presented as Table 1. The position of each penetration at each station is located on Figures 6a-g.

INTERPRETATION OF OBSERVATIONS

The east west suite of heat flow stations were deliberately run on the southern end of the distal fan to avoid problems of penetrating the very sandy sediments associated with the most recent turbidite flows on the Bengal Fan (Geller et al.,1983). We choose the line sufficiently far south that we avoided these sediments. However, the sediment thickness along the line varied markedly. The five westerly sites were on a thick uniform blanket of sediment. The two easterly sites were on a very thin sediment cover (show single channel water gun line here, Figure 7).

The five easterly sites show little scatter and have median values ranging from 58 to 67 mw/m2. The lowest value is from RC2707 DHF15. However, the small number of values makes the median somewhat suspect. There is little or no evidence from these five stations for any difference in heat flow (Figure 8a-e).

The two easterly sites in rougher topography show more scatter with hints of a bimodal distribution. These values are typical of values observed in areas affected by water flow in the crust. As a result of the large scatter the median value at these two stations cannot be differentiated from those to the west (Figure 8 f and g).

The heat flow values on the well sedimented ocean floor on the east west transect form a close group around 65 mw/sq. m. (Figure 9a). This value is close to that expected for ocean floor between 60 and 65 MA. These values should produce another datum point on the heat flow versus age relation for normal ocean floor.

The heat flow data on the region of little sediment cover show considerable scatter. When summed together there is a strong indication of a bimodal ditribution (Figure 9b). Such a distribution is typical of areas where hydrothermal convection cells are active in the oceanic crust. However, the water flow in the crust does not seem to affect the overall heat loss from these regions as the mean value is the same as the value observed on well sedimented crust. Thus, there is probaly little hydrothermal flow through the sediments between the crust and the ocean floor.

The major objective of the heat flow survey was to investigate if there was a correlation between the lineated geoid anomaly trends running NNE-SSW through the area and the heat flow. We have plotted the median heat flow values and the observed range of values at each station on projections of the geoid and shear wave travel time anomalies (figure 10).

We observed no significant variation in heat flow associated with either the geoid or travel time anomalies. If there is any correlation at all, it appears to be a slight inverse correlation to the geoid anomalies,

In summary we found that within the scatter in the heat flow data (10 mw/sq. m.) there is no evidence that the lithospheric plate has been heated perpendicular to the direction of motion. It appears that small scale convection in the upper mantle can be ruled as an explanation of the heat flow anomalies in the area as a whole.

TABLE 1

STATION	LATITUDE S	LONGITUDE E	DEPTH m	PEN m	Np	GRADIENT mK/m	K W/m-K	Q mW/m^2	ST.DEV. EVALUATION mW/m^2	
									0	
DHF 12A	7 00.00'	78 57.12'	5292	4.4	5	88	.76	67	1	10 Mean
B	6 59.99'	78 56.16'	5288	3.9	4	88	.76	67	2	10 66.8952
C	6 59.85'	78 56.83'	5285	3.8	6	90	.76	68	3	10 St.Dev.
D	6 59.84'	78 56.40'	5280	3.9	6	94	.76	72	4	9 5.2079320
E	6 59.25'	78 55.83'	5265	3.7	6	98	.76	74	3	10 N
F	6 59.60'	78 55.18'	5271	4.2	6	88	.76	67	3	9 10
G	6 59.80'	78 54.38'	5261	3.7	6	91	.76	69	5	9
H	6 59.68'	78 53.76'	5255	4.5	5	72	.76	55	4	8
I	7 00.02'	78 52.98'	5245	3.5	4	89	.76	67	7	8
J	7 00.00'	78 52.44'	5241	3.8	3	83	.76	63	11	7
DHF 13A	7 00.55'	79 44.34'	5025	3.7	4	86	.76	65	1	8 Mean
B	6 59.68'	79 44.87'	5028	3.2	4	89	.76	68	3	9 63.1864
C	7 00.44'	79 45.33'	5006	3.6	4	82	.76	62	5	8 St.Dev.
D	7 00.36'	79 45.43'	5007	3.3	4	88	.76	67	4	8 2.6896795
E	7 00.16'	79 46.20'	4992	3.2	3	82	.76	62	1	7 N
F	7 00.04'	79 46.86'	4988	3.9	5	80	.76	61	3	9 10
G	6 59.99'	79 47.40'	4980	3.2	4	85	.76	65	5	8
H	7 00.03'	79 47.90'	4967	3.4	4	83	.76	63	2	8
I	7 00.00'	79 48.63'	4958	3.8	5	79	.76	60	4	8
J	7 00.04'	79 49.20'	4945	3.7	5	79	.76	60	1	10
DHF 14A	7 01.01'	80 45.18'	5041	3.9	6	87	.79	68	1	10 Mean
B	7 00.17'	80 45.90'	5041	4.1	6	89	.79	71	2	10 66.484143
C	7 00.30'	80 46.48'	5037	4.1	6	88	.79	69	3	10 St.Dev.
D	7 01.80'	80 46.84'	5030	3.8	7	91	.79	72	2	10 5.5071831
										N
V36 64A	6 53.90'	80 48.10'	5054		5	81	.79	64	0	8 14
B	6 52.90'	80 47.60'	5064		5	86	.79	68	0	8
C	6 52.10'	80 47.50'	5066		5	81	.79	64	0	8
D	6 51.80'	80 47.20'	5058		5	74	.79	59	0	8
E	6 50.90'	80 46.80'	5060		5	84	.79	66	0	8
F	6 49.70'	80 46.60'	5015		5	72	.79	57	0	8
G	6 49.10'	80 45.10'	5043		5	77	.79	61	0	8
H	6 48.50'	80 45.30'	5062		5	81	.79	64	0	8
I	6 47.30'	80 45.10'	5103		4	89	.79	70	0	7
J	6 46.10'	80 44.70'	5121		5	98	.79	78	0	8
DHF 15A	7 00.27'	81 35.34'	4892	3.8	6	72	.79	57	3	9 Mean
B	7 00.50'	81 36.82'	4887	3.6	5	70	.79	55	1	8 56.394714
C	7 00.30'	81 36.59'	4815	3.6	4	74	.79	59	0	8 St.Dev.
D	7 00.35'	81 37.23'	4810	1	2	0	.79			0 1.9131644
E	7 00.42'	81 37.24'	4816	1.2	3	0	.79			0 N
F	7 00.48'	81 37.25'	4816	1	2	0	.79			0 7
G	7 00.54'	81 37.27'	4816	0	0	0	.79			0
H	7 00.06'	81 38.61'	4831	3.9	4	72	.79	57	3	8
I	6 59.77'	81 39.26'	4830	4	3	74	.79	59	2	7
J	7 00.37'	81 40.15'	4818	3.9	4	69	.79	54	3	7
K	7 00.36'	81 40.75'	4822	3.8	4	68	.79	54	3	7
DHF 16A	7 00.20'	82 17.70'	4900	3.7	4	84	.79	67	5	7 Mean
B	6 59.94'	82 18.56'	4907	3.7	5	79	.79	62	3	8 65.009818
C	6 59.97'	82 19.07'	4906	3.6	5	92	.79	73	2	9 St.Dev.
D	6 59.98'	82 19.73'	4918	4	7	69	.79	54	2	9 7.2938398
E	6 59.82'	82 21.29'	4921	3.9	5	80	.79	63	4	8 N
F	7 00.26'	82 20.84'	4927	3.5	4	85	.79	67	2	8 11

G	7 00.10' 82 21.36'	4937	3.9	4	79	.79	62	1	9
H	7 00.18' 82 22.27'	4927	3.9	5	95	.79	75	3	10
I	6 59.87' 82 22.77'	4922	3.5	4	78	.79	61	1	8
J	7 00.28' 82 23.50'	4907	3.5	4	96	.79	76	3	8
K	7 00.10' 82 24.06'	4883	3.6	4	70	.79	55	1	8
OHF 17A	7 00.05' 83 06.82'	4890	3.9	5	89	.77	69	1	10 Mean
B	6 59.95' 83 07.34'	4874	3.4	5	96	.77	74	2	10 63.336
C	6 59.92' 83 07.85'	4851	3.4	4	110	.77	85	1	9 St.Dev.
D	7 00.08' 83 08.35'	4845	3.2	4	103	.77	79	3	9 14.775831
E	7 00.02' 83 09.02'	4861	3.7	6	108	.77	83	2	10 N
F	7 00.20' 83 09.45'	4852	3.7	7	68	.77	52	1	10 11
G	7 00.25' 83 10.01'	4885	3.4	5	77	.77	59	1	10
H	7 00.00' 83 10.70'	4908	3.9	6	64	.77	50	1	10
I	6 59.95' 83 11.31'	4914	3.7	5	65	.77	50	4	8
J	7 00.02' 83 11.90'	4914	3.2	5	65	.77	50	3	8
K	7 00.53' 83 12.58'	4899	3.4	4	60	.77	47	2	7
L	7 00.40' 83 13.10'	4902	3.4	4	80	.77	62	0	8
OHF 18A	7 00.03' 83 56.31'	4902	3.9	4	70	.77	54	1	8 Mean
B	7 00.02' 83 57.04'	4890	3.5	3	101	.77	77	1	8 69.933111
C	7 00.02' 83 57.48'	4883	3.3	3	90	.77	69	1	7 St.Dev.
D	7 00.01' 83 57.99'	4904	2.7	3	113	.77	87	2	8 9.8635000
E	6 59.98' 83 59.55'	4915	3.5	3	81	.77	62	1	7 N
F	7 00.03' 83 59.19'	4916	3.5	4	98	.77	76	4	8 9
OHF 19A	7 00.29' 83 59.98'	4914	3.7	4	87	.77	67	1	8
B	6 59.99' 84 00.60'	4911	4.3	3	81	.77	62	2	7
C	7 00.04' 84 01.59'	4901	1	2	0	.77			0
D	7 00.04' 84 01.59'	4901	3.4	2	98	.77	75	4	6
OHF 20A	17 05.11' 88 05.11'	1704	0	0	0				0
B	17 05.11' 88 07.52'	1704	0	0	0				0
C	17 05.12' 88 07.53'	1704	0	0	0				0
D	17 05.10' 88 08.17'	1712	0	0	0				0
E	17 05.11' 88 08.22'	1712	0	0	0				0
F	17 05.13' 88 08.26'	1712	0	0	0				0
OHF 21A	17 05.50' 88 06.89'	1711	0	0	0				0
B	17 05.51' 88 06.88'	1711	0	0	0				0

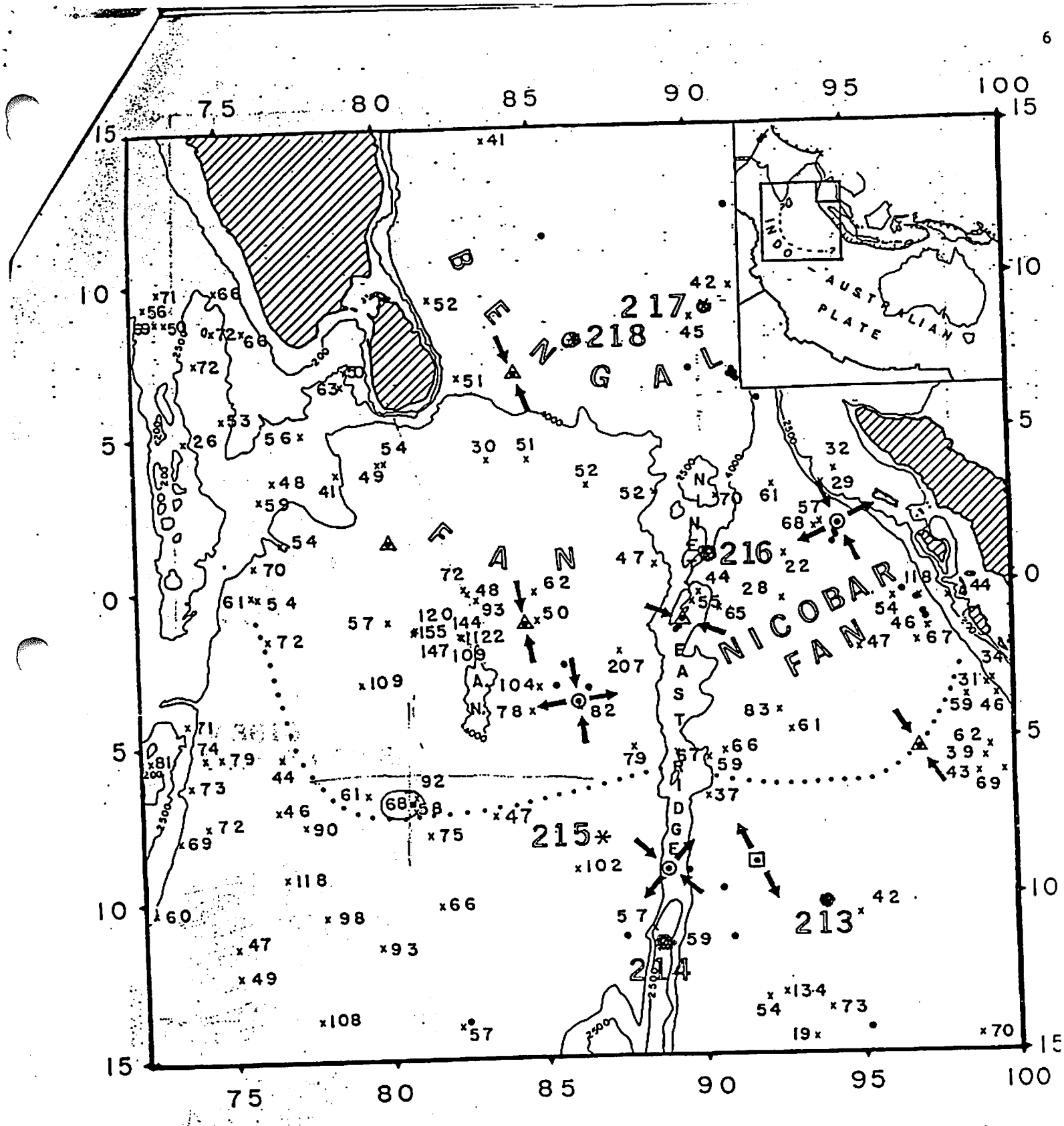

Fig. 2. Crosses denote the locations of heat flow measurements (in mWm^{-2}) compiled by Geller et al., (1983). The small square at the southern end of the Bengal Fan is the average heat flow from site 64. Asterisks indicate DSDP locations. A.N. is Afanazy Nikitan seamount group. Solid dots are intraplate earthquakes. Triangles denote thrust focal mechanisms, circles strike slip mechanisms, and square normal mechanisms. The dotted lines roughly show the southern limit of fan deposits. The dashed line in the upper right hand corner is the southern limit of the observed deformation. Strikes of principal stress axes for intraplate earthquakes within the Indo-Australian plate are shown by arrows. Depths are contoured in m.

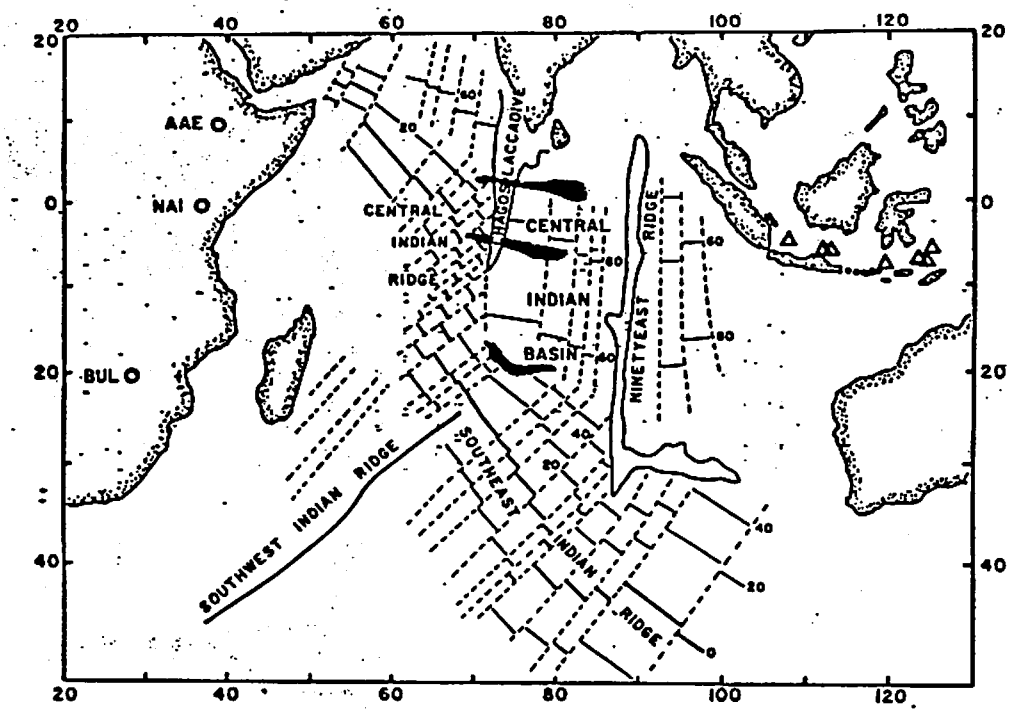

Fig. 2 Earthquake (triangles) and station locations (circles), with plate boundaries and tectonic features of study area. Shading covers areas sampled by surface bounce points. AAE is the WWSSN station at Addis Ababa, Ethiopia; NAI is at Nairobi, Kenya; and BUL is at Bulawayo, Zimbabwe. Northernmost shaded area represents bounce points for ray paths to AAE, central area represents paths to NAI, and southern area represents paths to BUL. Dashed lines represent fracture zones. Isochrons and plate boundaries are from Anderson et al. (1977), with ages shown in millions of years.

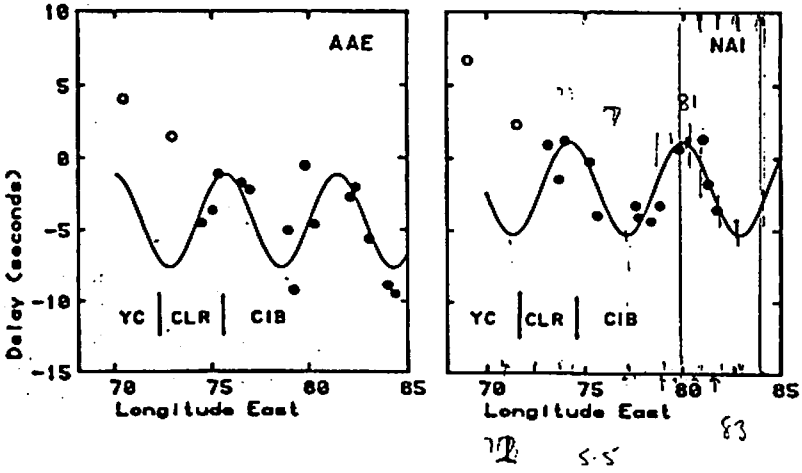

Fig. 3 PEM-C residuals versus longitude. Solid curves are best-fitting sinusoid to Central Indian Basin points. YC, young crust; CLR, Chagos-Laccadive Ridge; CIB, Central Indian Basin. Filled dots are data from CIB and eastern half of CLR used in the inversion for sine waves.

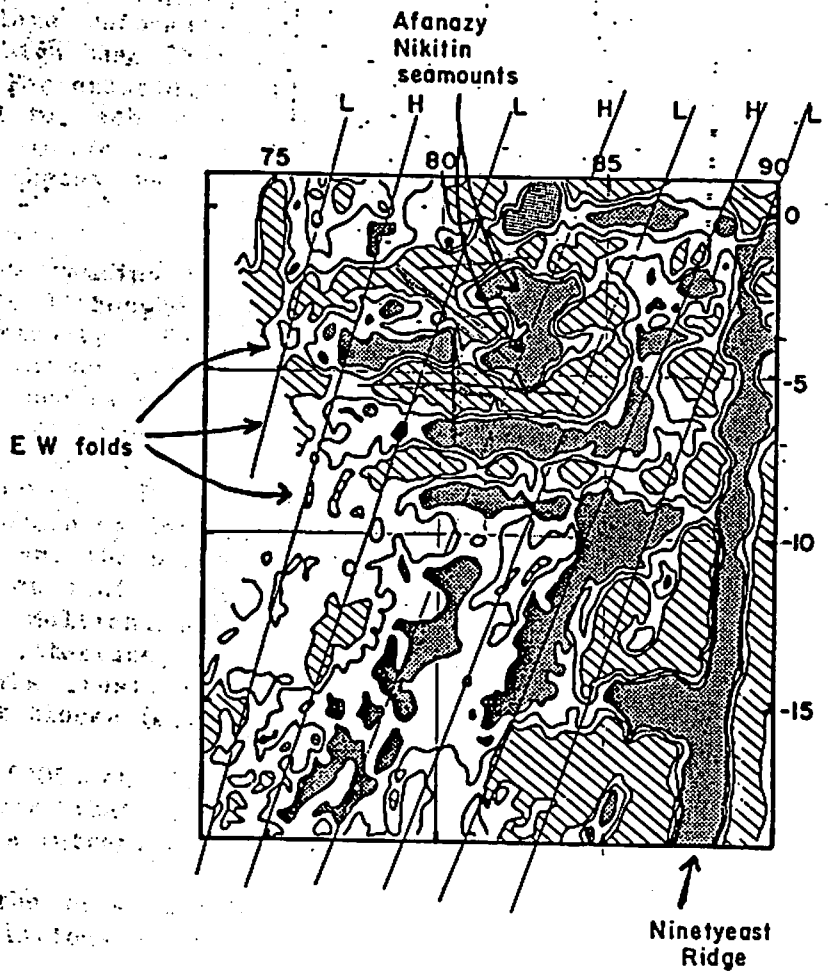

Fig. 3. Seasat-derived gravity anomalies in the Central Indian Ocean (from Weissel and Haxby 1982; 1984). Shaded areas, +7.5 mgals or greater; lined areas, -7.5 mgals or less. The zero contour is also shown. Note alternating bands of highs (H) and lows (L) trending roughly N15°E.

THERMAL CONDUCTIVITY

East-West Transect, RC27-07

Core 70 Core 71 Core 72

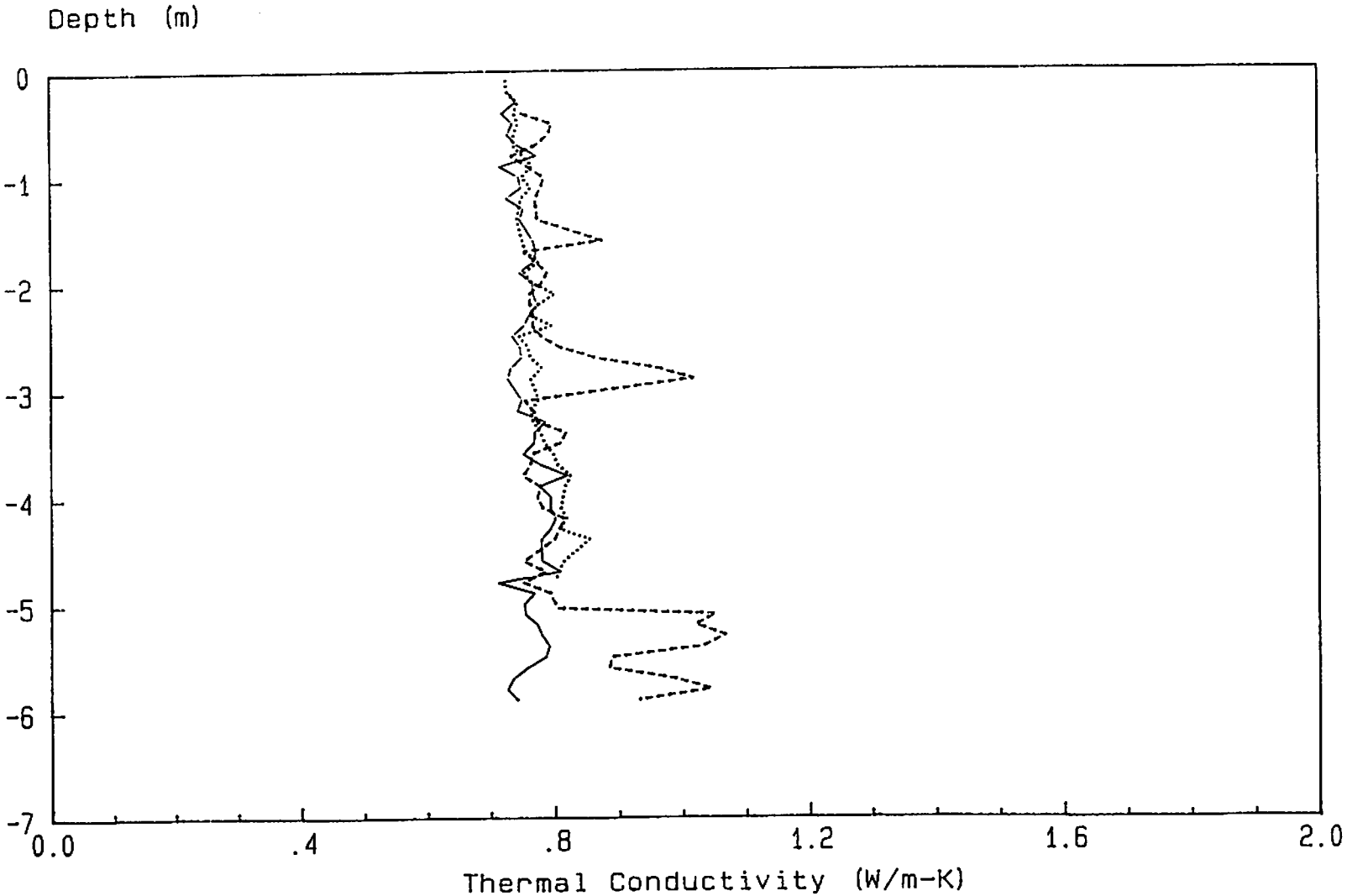

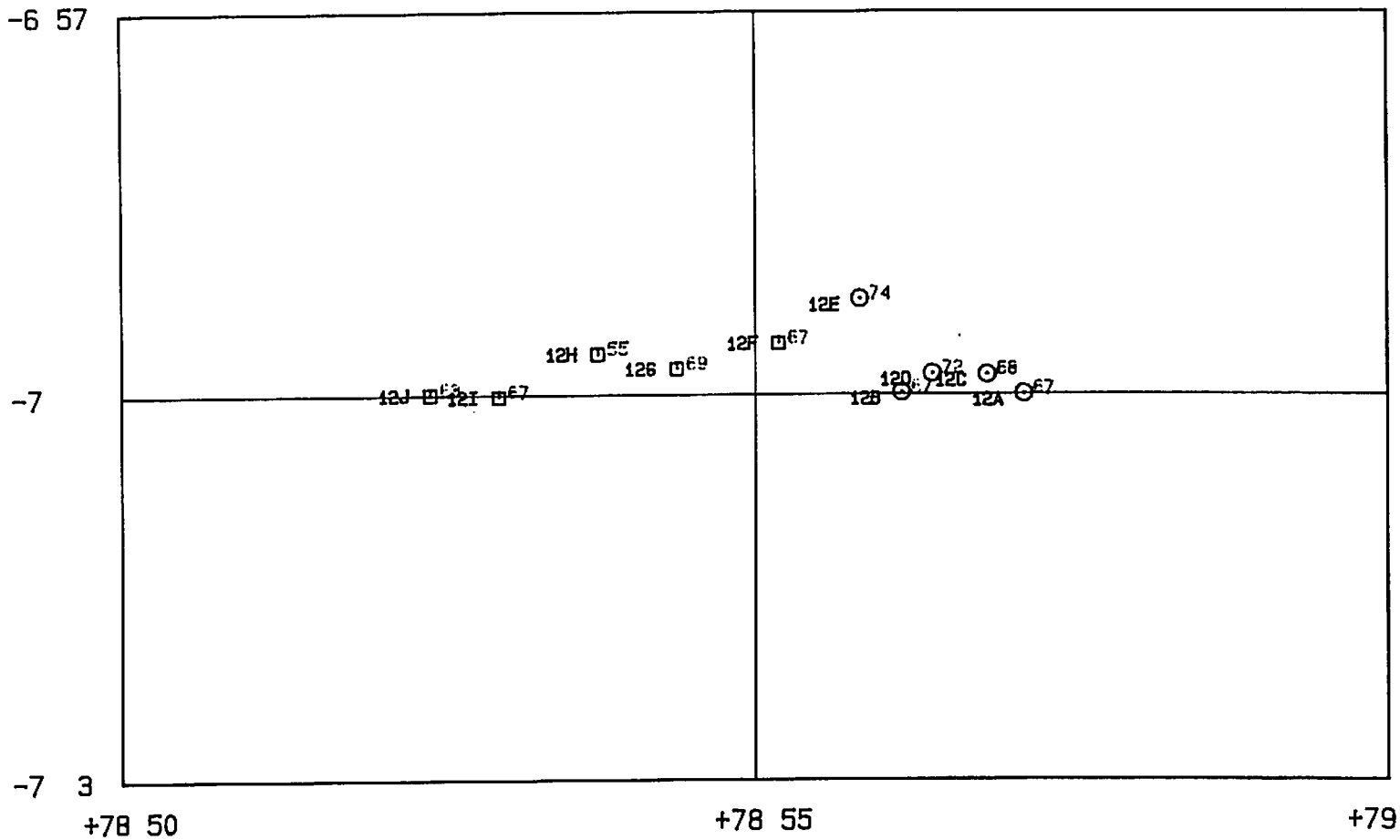

Scale 1: 100000

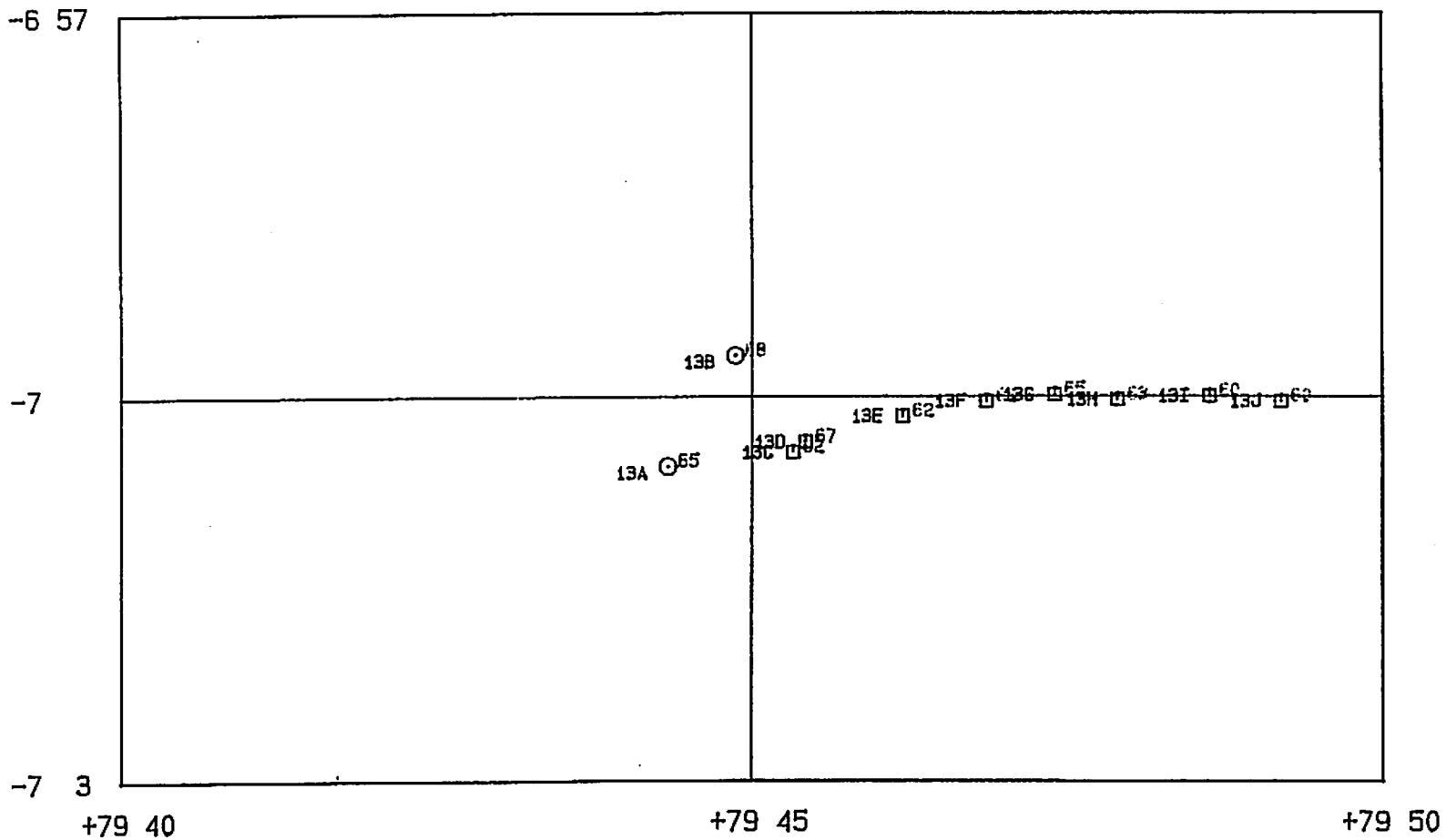

Scale 1: 100000

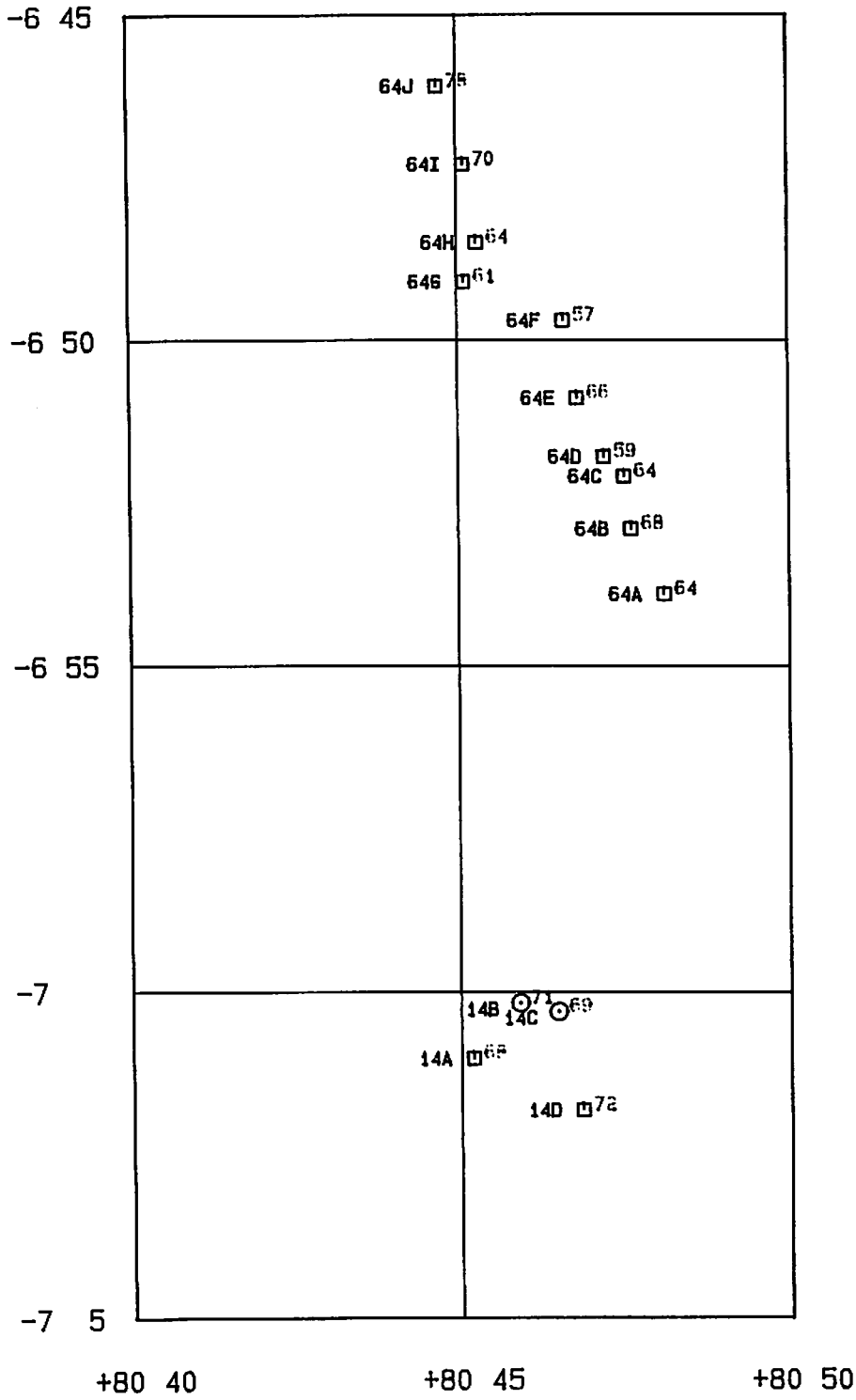

Scale 1: 200000

6c

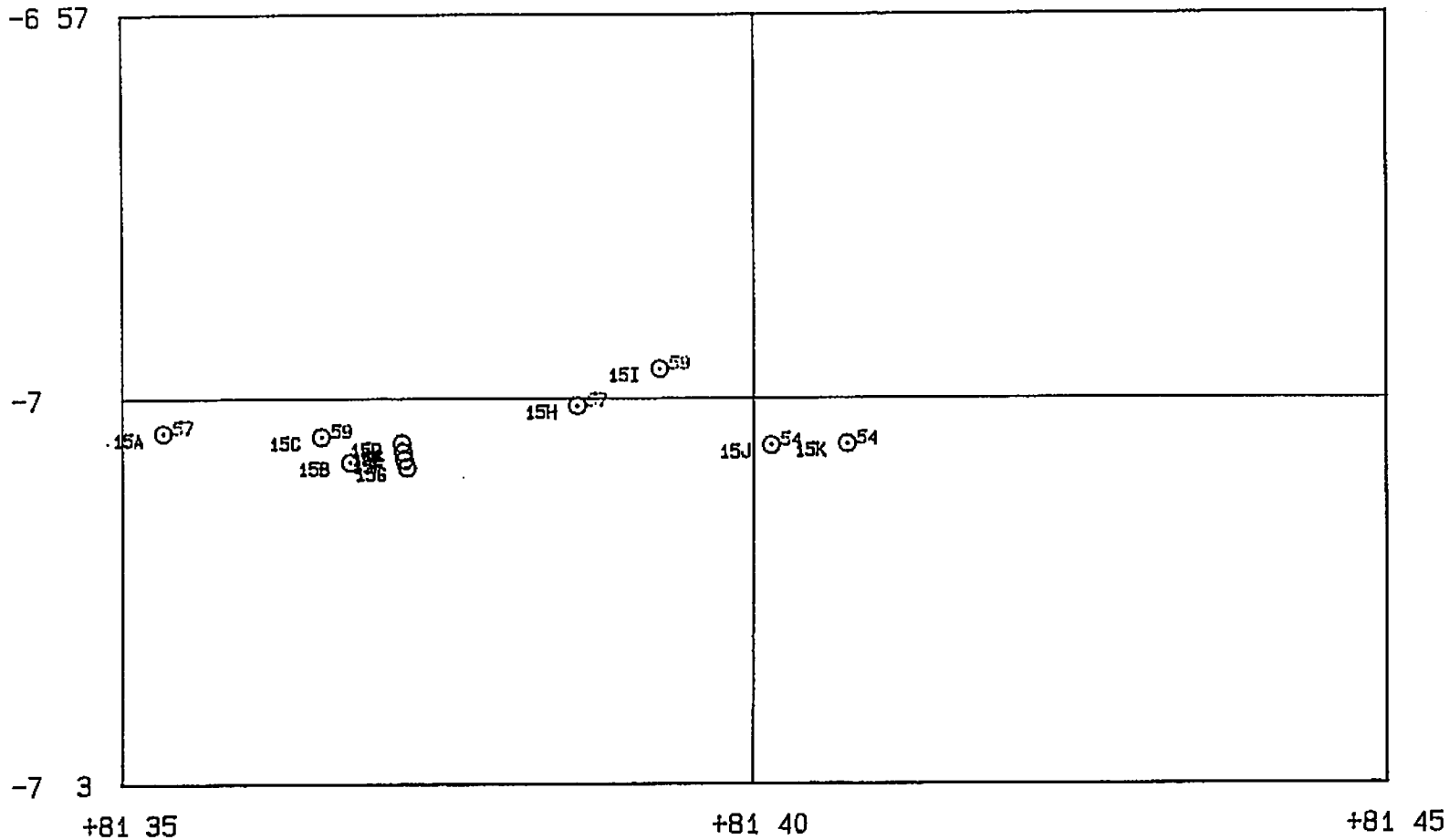

Scale 1: 100000

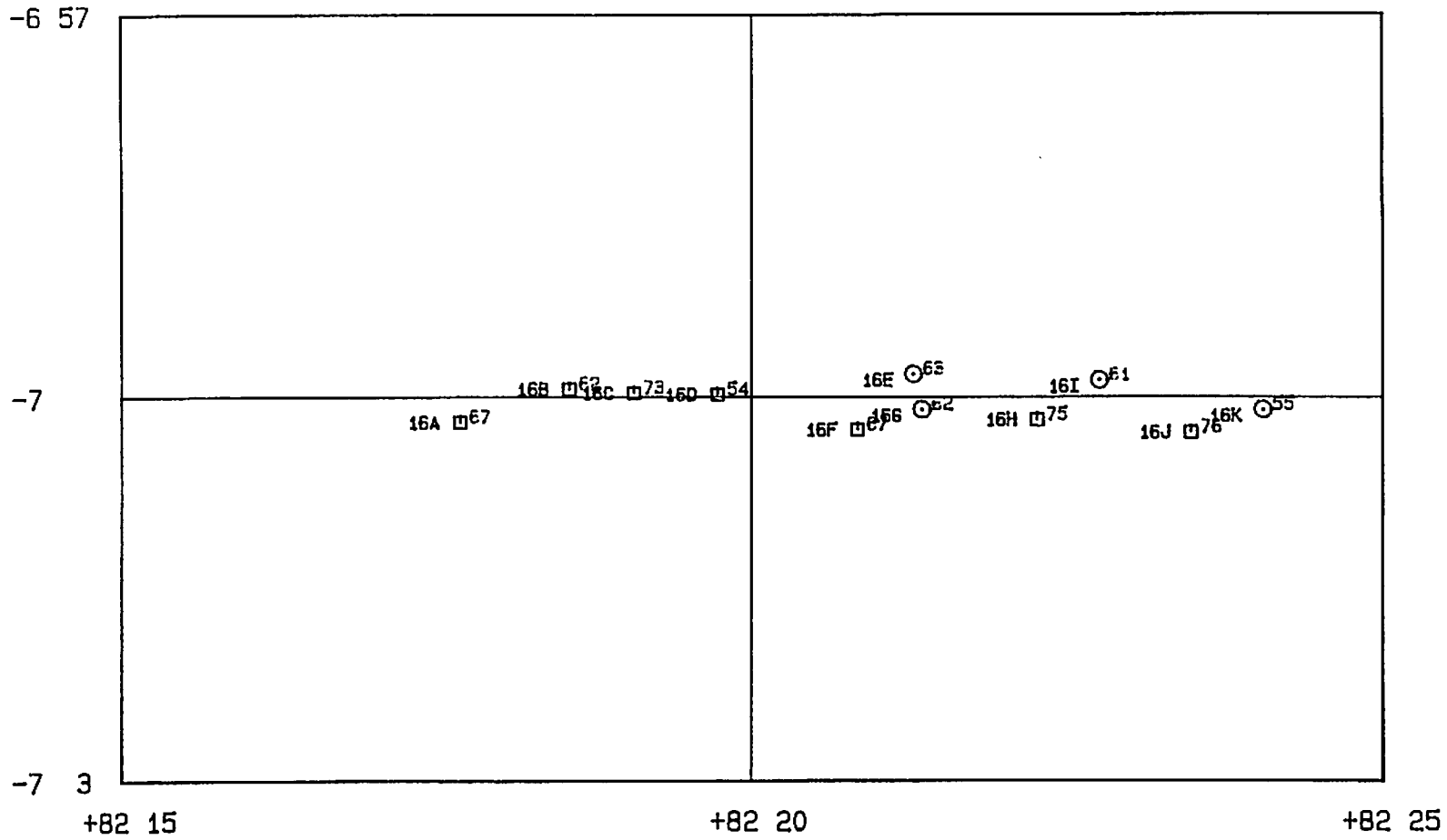

Scale 1: 100000

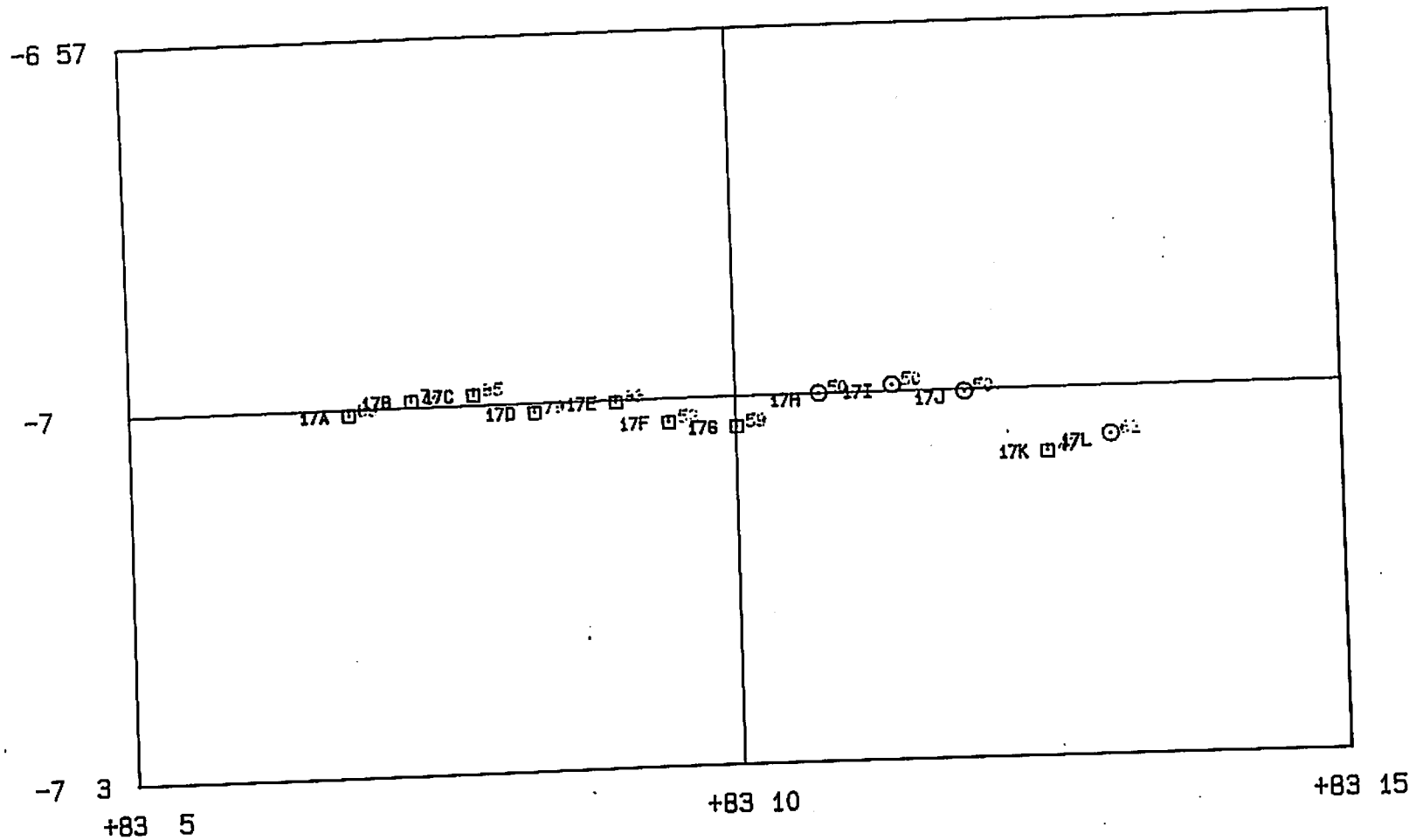

Scale 1: 100000

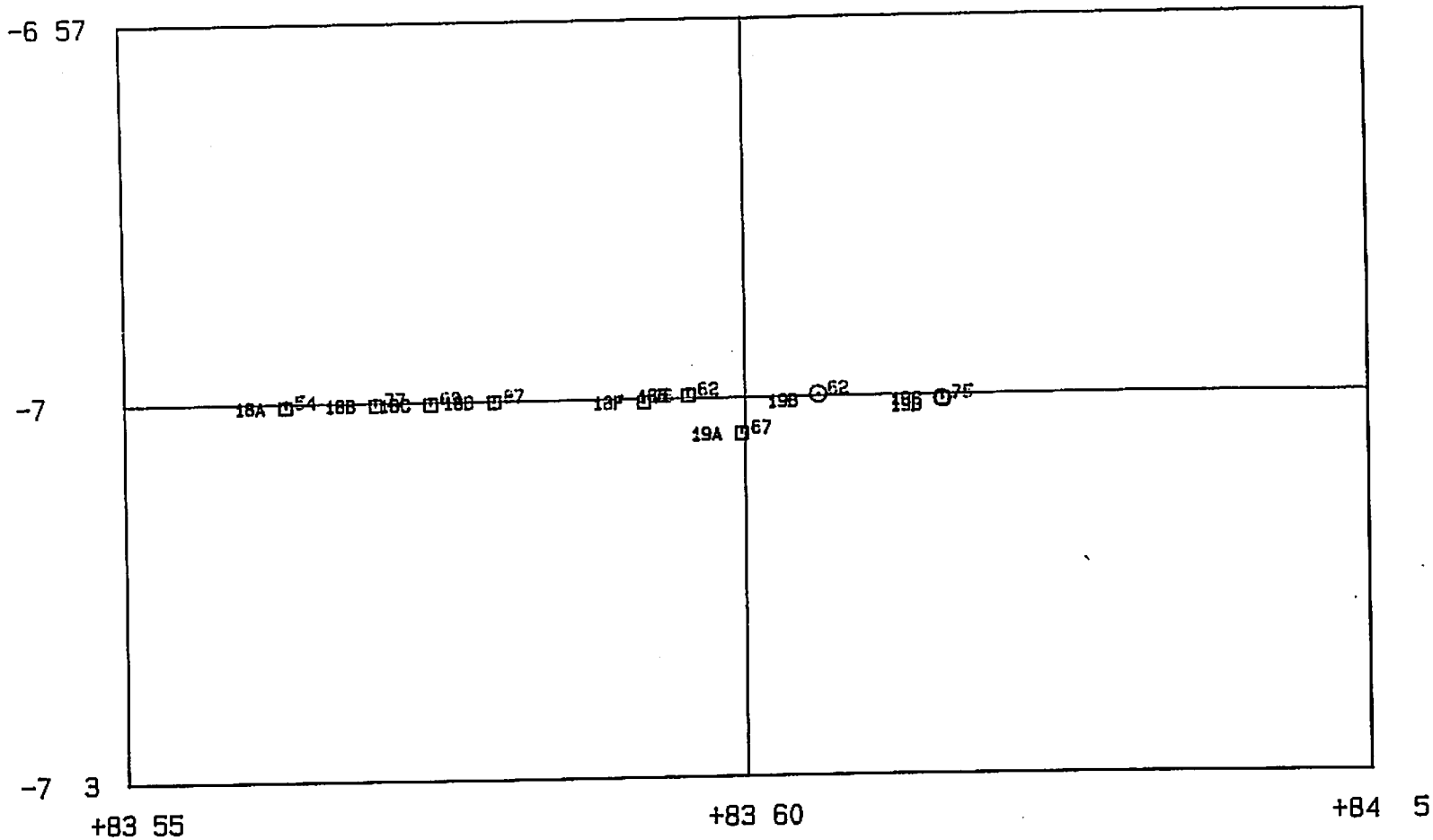

Scale 1: 100000

Figure 7

Seismic Section with heat flow stations superimposed.

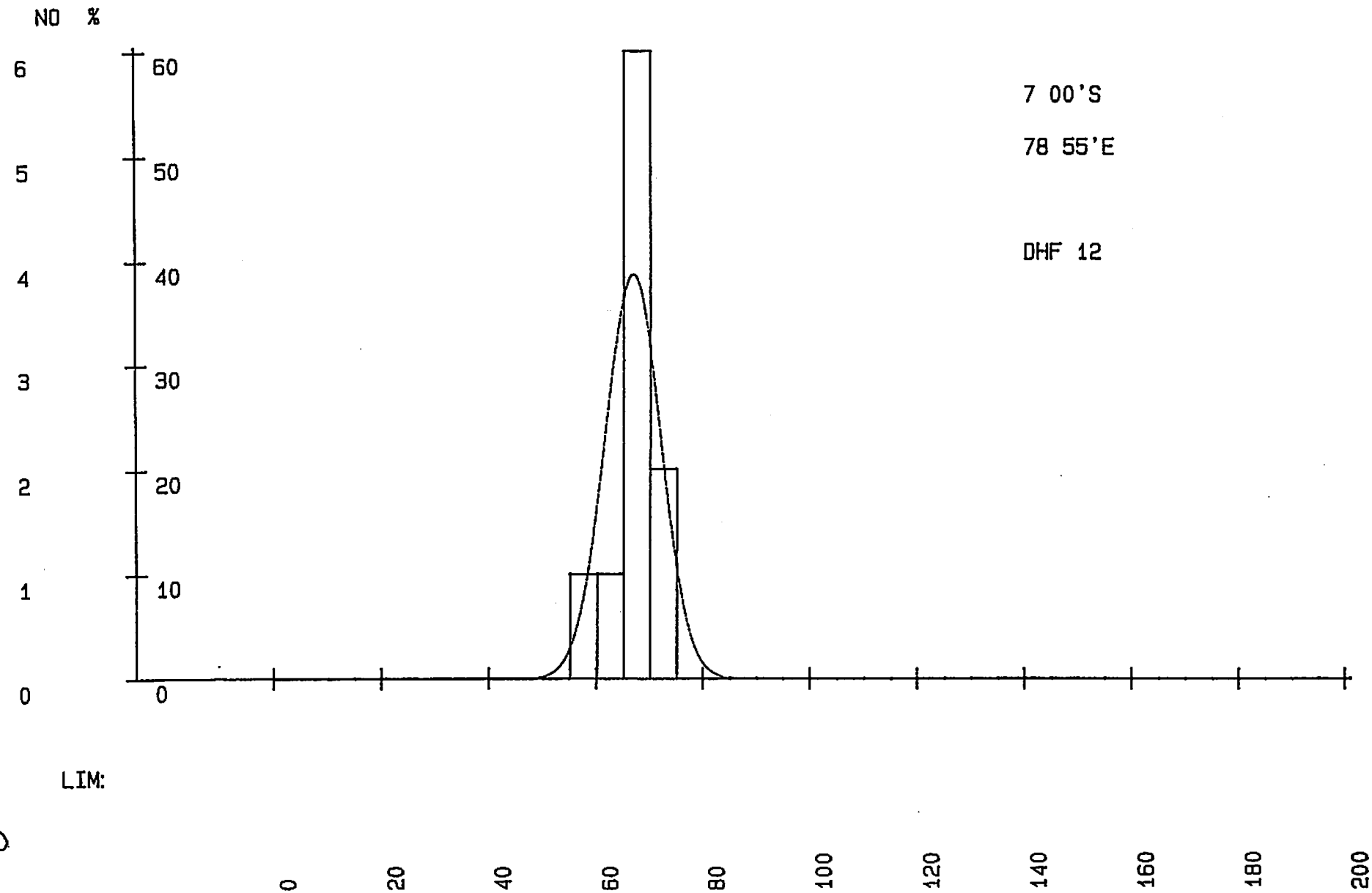
NO %
6
5
4
3
2
1
0
60
50
40
30
20
10
0
7 00'S
78 55'E
DHF 12
LIM:
0
20
40
60
80
100
120
140
160
180
200

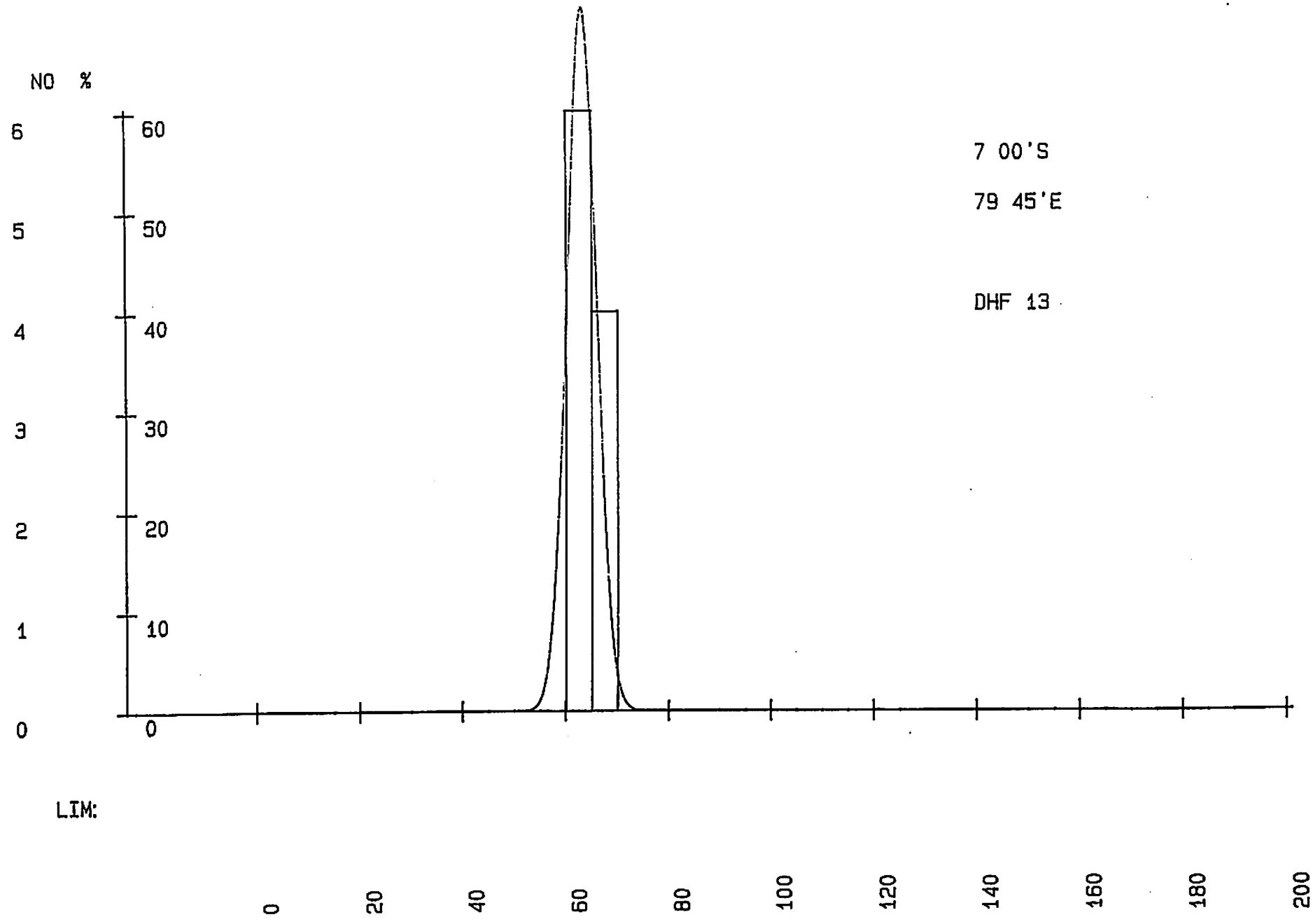
NO %
6
5
4
3
2
1
0
60
50
40
30
20
10
0
7 00'S
79 45'E
DHF 13
LIM:
0
20
40
60
80
100
120
140
160
180
200

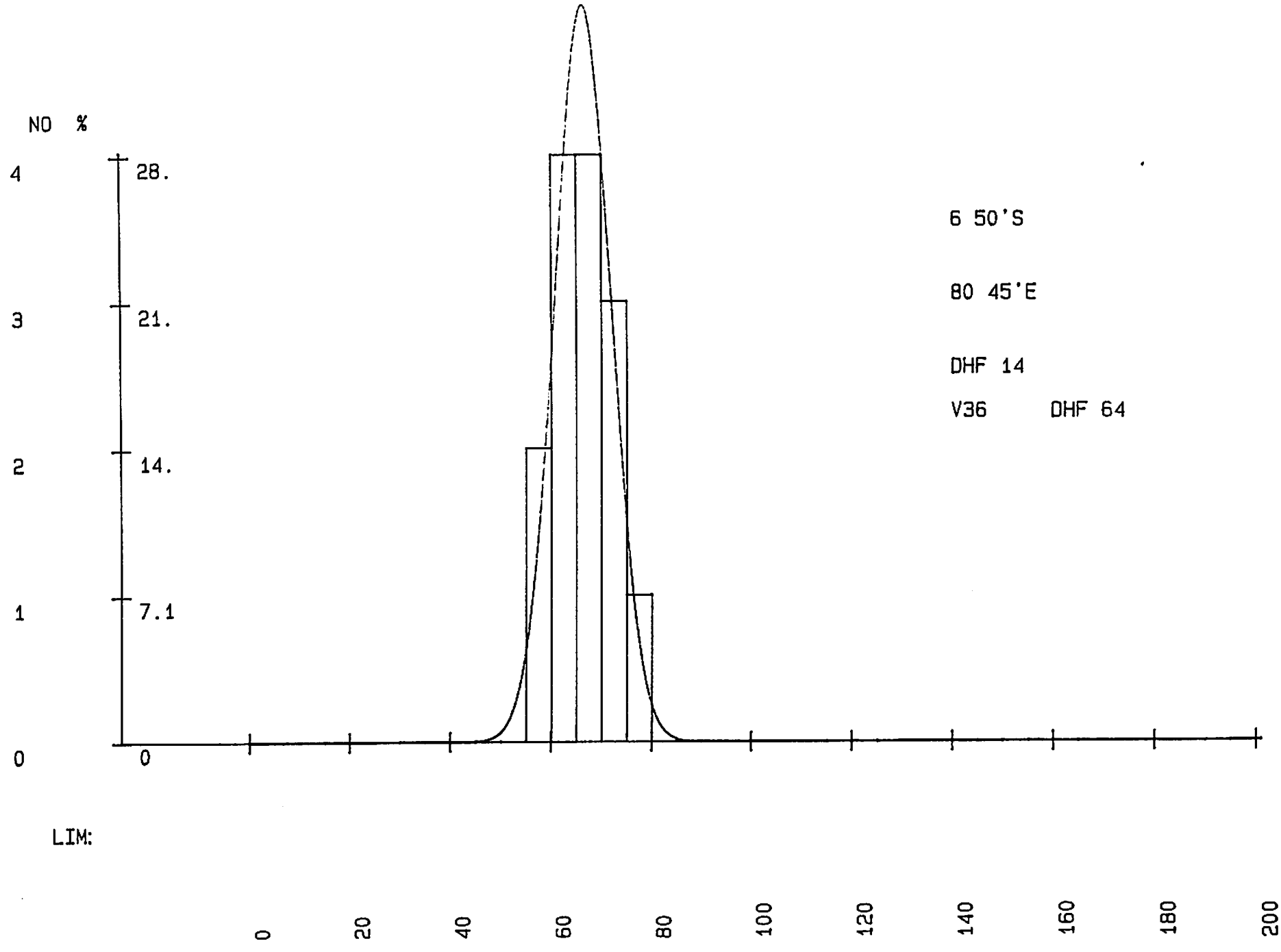
NO %
4
3
2
1
0
28.
21.
14.
7.1
0
6 50'S
80 45'E
DHF 14
V36 DHF 64
LIM:
0
20
40
60
80
100
120
140
160
180
200

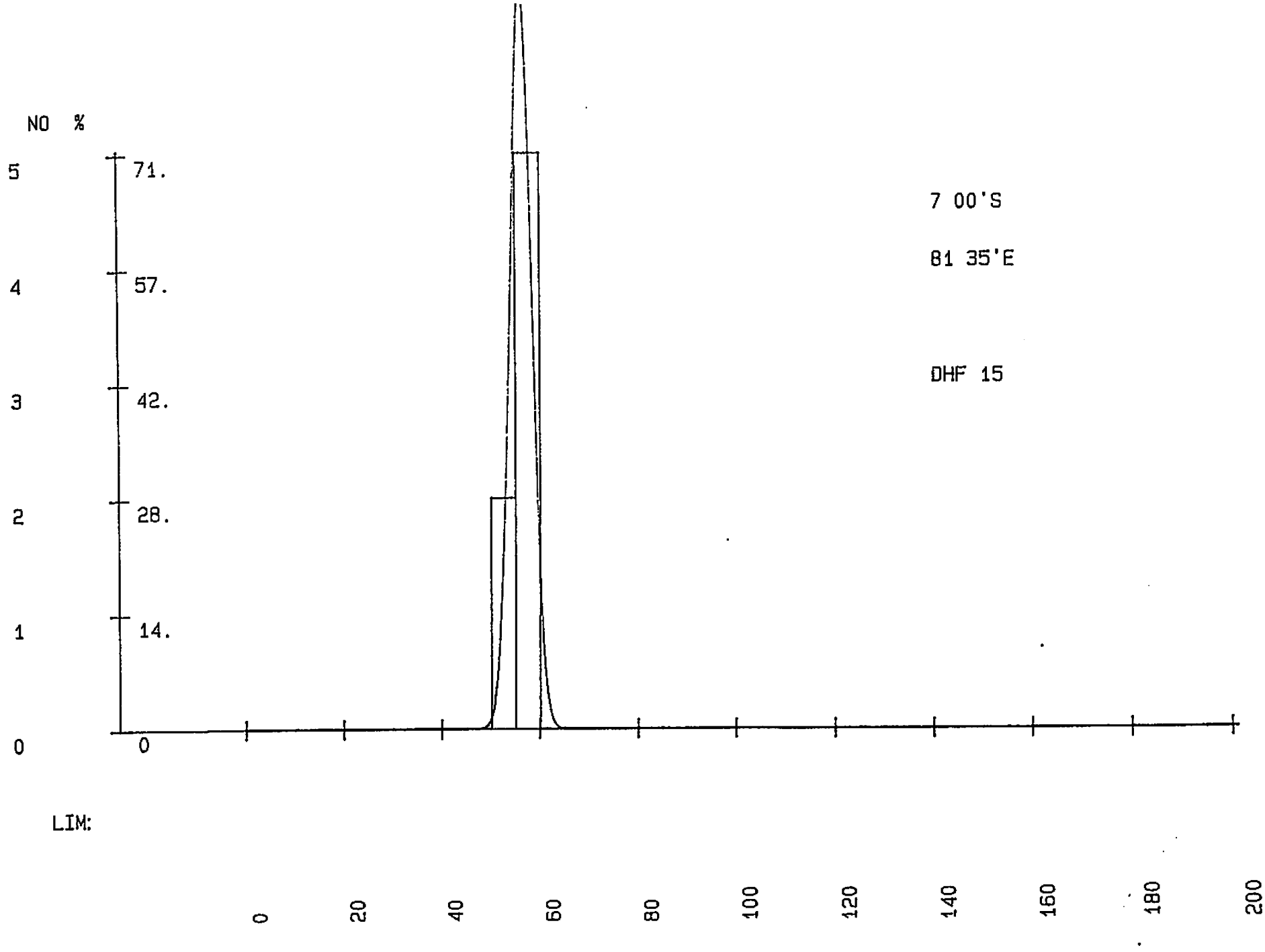
NO %
5
4
3
2
1
0
71.
57.
42.
28.
14.
0
7 00'S
81 35'E
DHF 15
LIM:
0
20
40
60
80
100
120
140
160
180
200

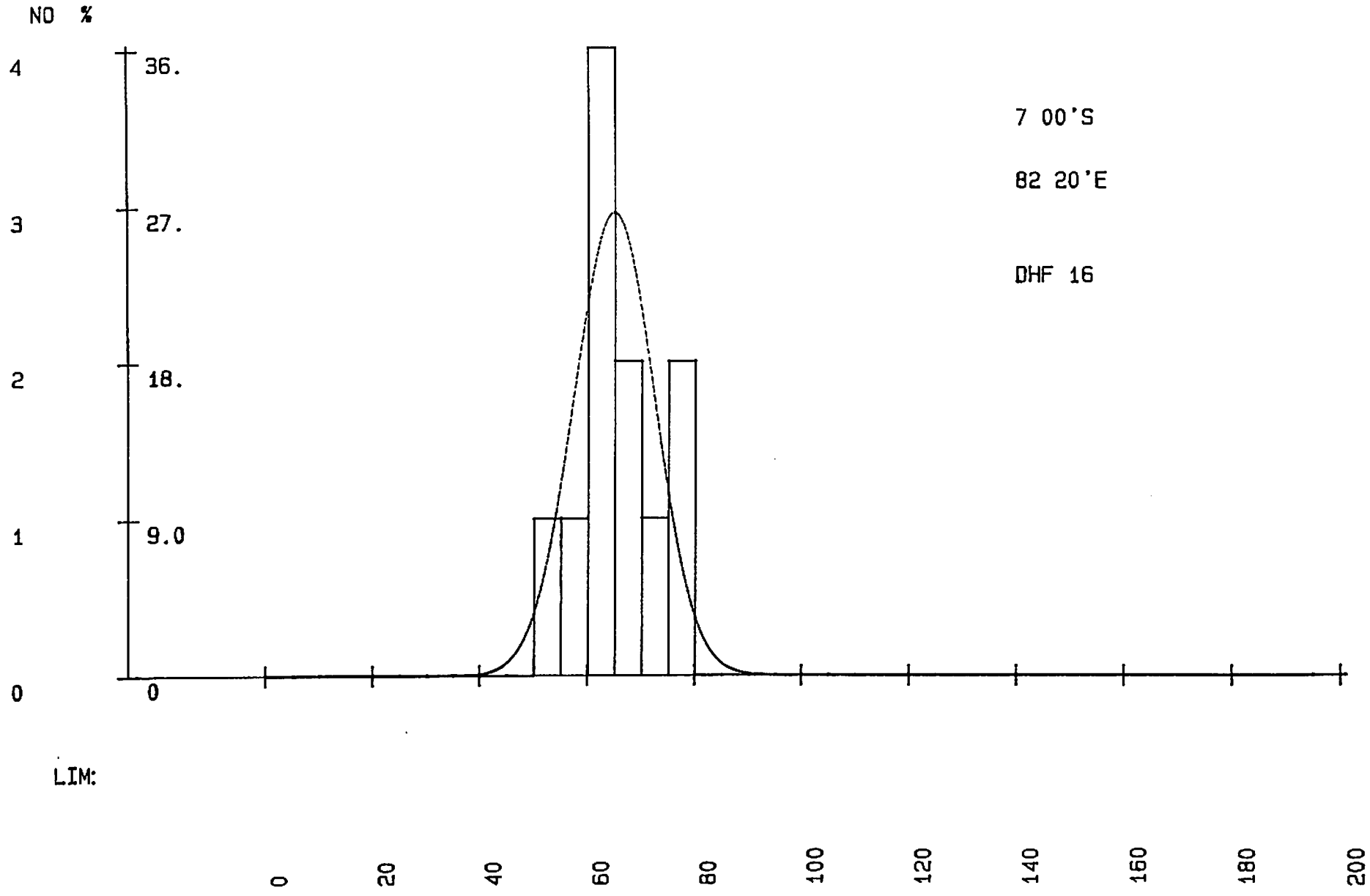
NO %
4
3
2
1
0
36.
27.
18.
9.0
0
7 00'S
82 20'E
DHF 16
LIM:
0
20
40
60
80
100
120
140
160
180
200

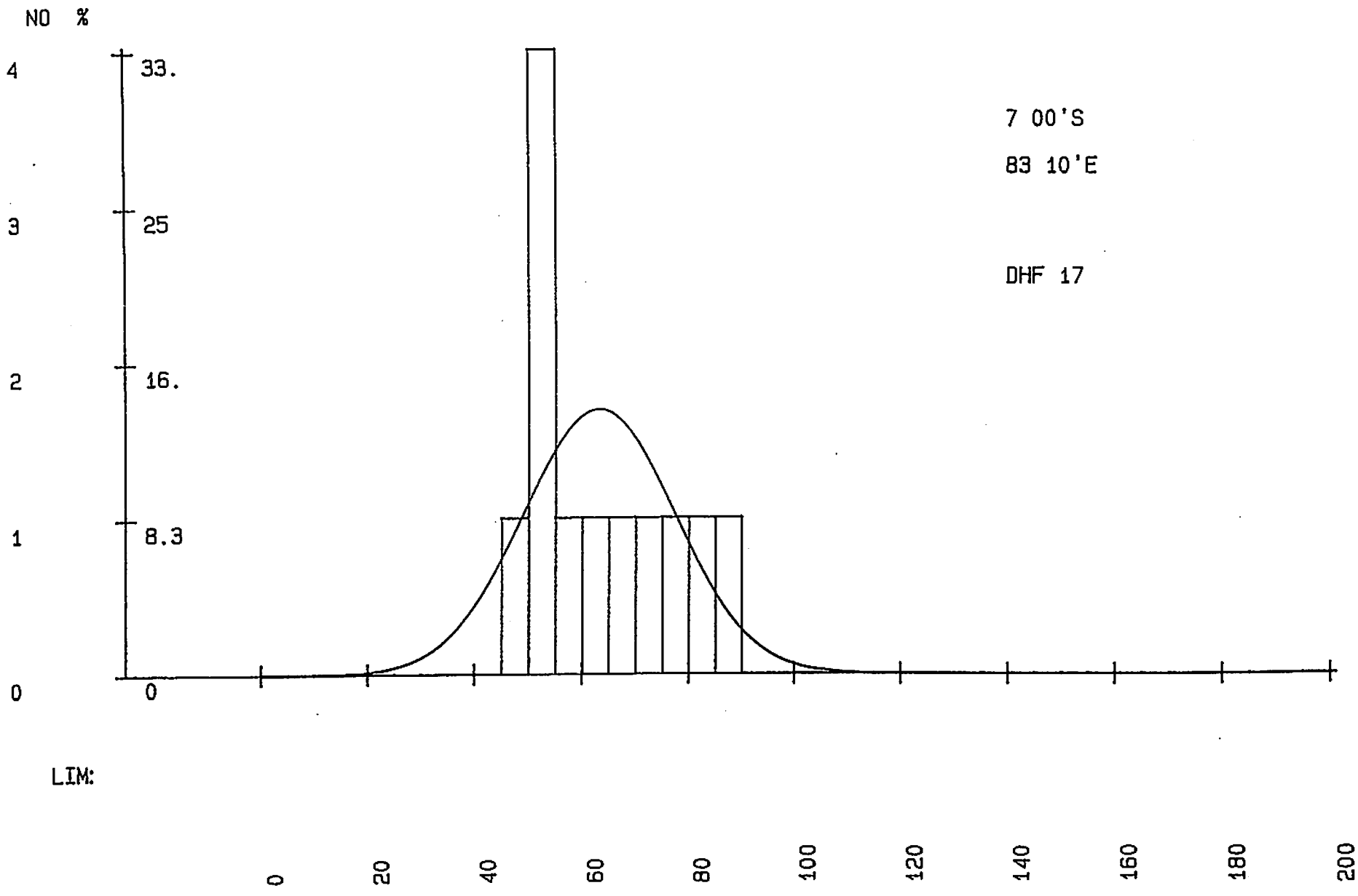
NO %
4
3
2
1
0
33.
25
16.
8.3
0
7 00'S
83 10'E
DHF 17
LIM:
0
20
40
60
80
100
120
140
160
180
200

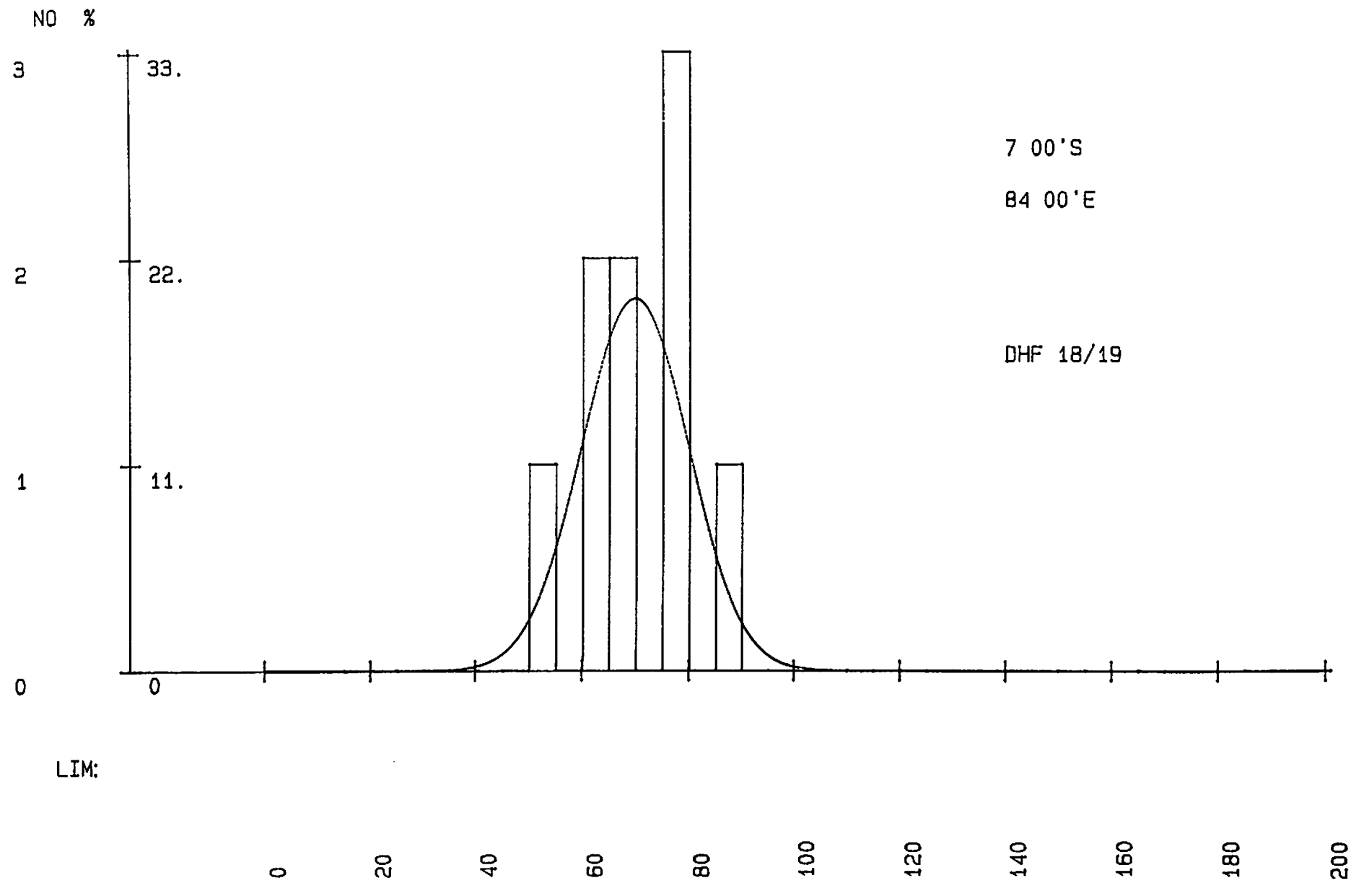
NO %
3
33.
2
22.
1
11.
0
0
7 00'S
84 00'E
DHF 18/19
LIM:
0
20
40
60
80
100
120
140
160
180
200

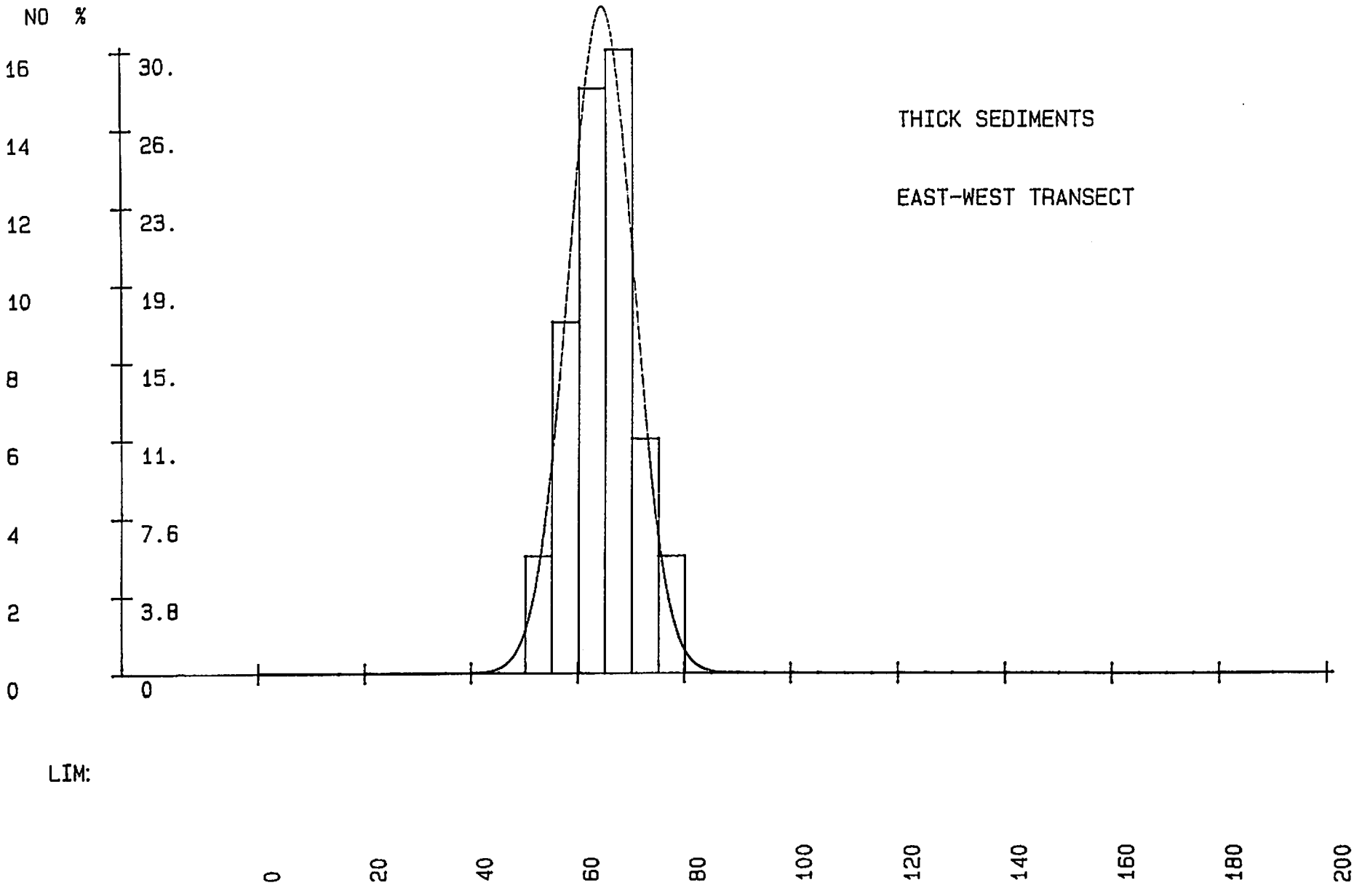
NO %
16
14
12
10
8
6
4
2
0
30.
26.
23.
19.
15.
11.
7.6
3.8
0
THICK SEDIMENTS
EAST-WEST TRANSECT
LIM:
0
20
40
60
80
100
120
140
160
180
200

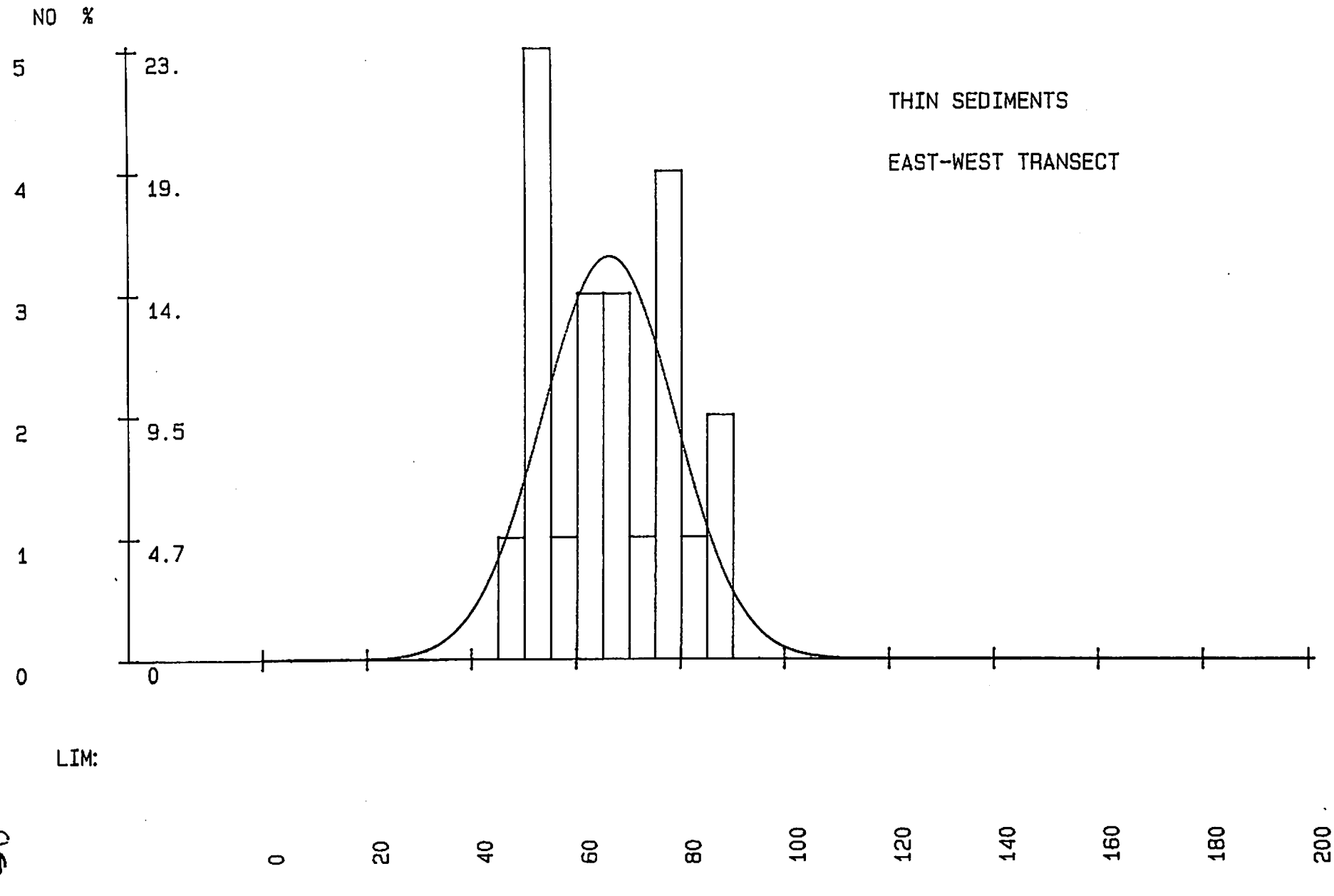
NO %
5
4
3
2
1
0
23.
19.
14.
9.5
4.7
0
THIN SEDIMENTS
EAST-WEST TRANSECT
LIM:
0
20
40
60
80
100
120
140
160
180
200

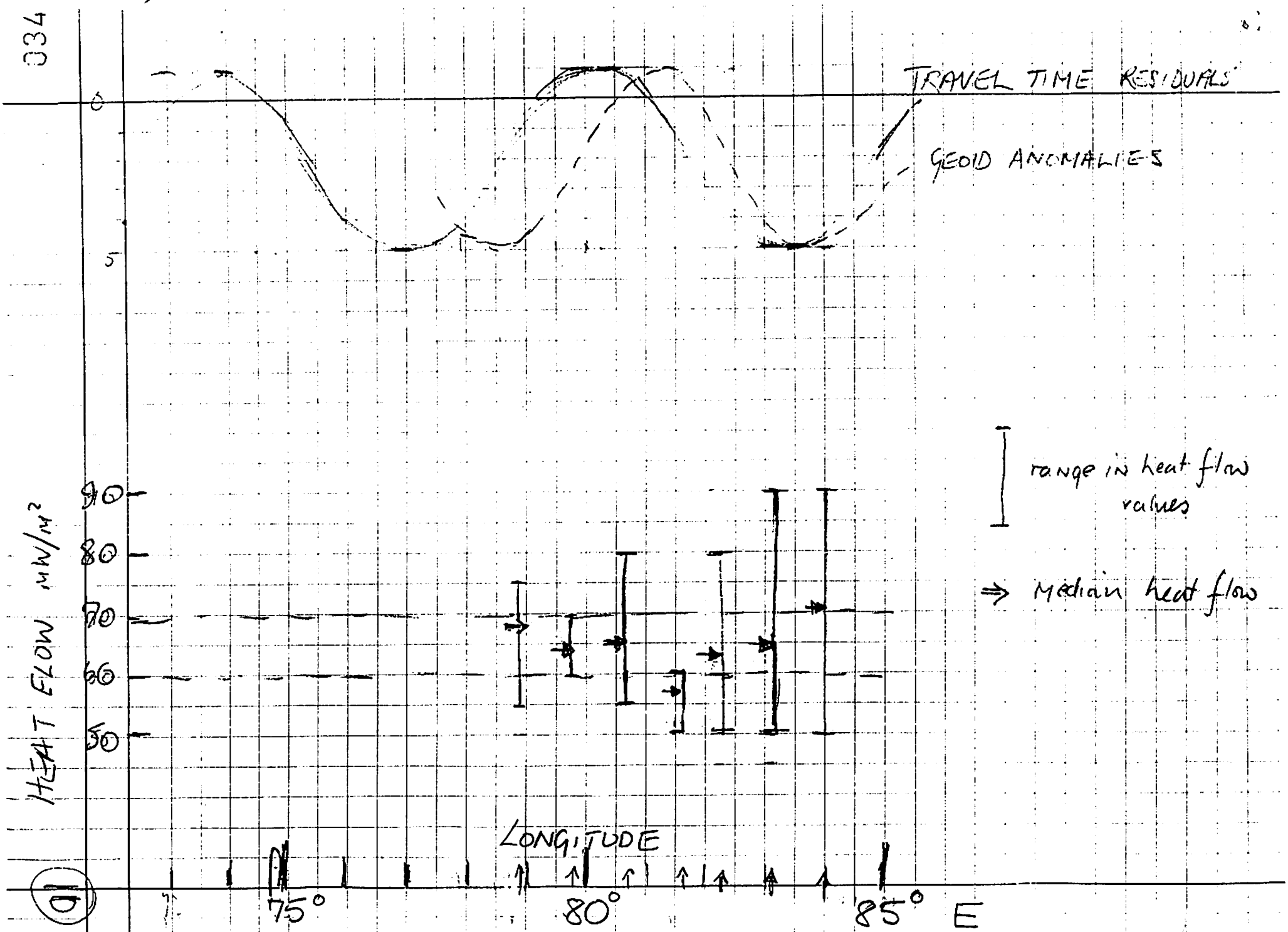
TRAVEL TIME RESIDUALS
GEOID ANOMALIES
0
5
range in heat flow values
⇒ Median heat flow
HEAT FLOW mW/m²
90
80
70
60
50
LONGITUDE
75°
80°
85° E

PART 2

RC 27-07

REPORT ON ODP SITE SURVEY AT

17°S 88°E

BY

JOHN G. SCLATER

AND

JIRI SAVRDA

At 17°S 88°E the Ninetyeast ridge trends NNE - SSW. It lies about 2500 m above the surrounding sea floor and is capped by 300 - 500 m of dominantly carbonate sediment.

For the purpose of selecting an ODP site we surveyed the area by running a digital single channel seismic survey over the top of the ridge. The lines were 15 Nm long and 2.5 Nm apart. We started by running east west lines and finished by running the three NNW - SSE lines. In addition to those three lines we ran a sonobuoy line using the water guns as a sound source.

In the center of survey area we took a core and attempted a multi-penetration heat flow station. The core was successful recovering 5 m of foraminiferous sand. The heat flow survey was spectacularly unsuccessful, however, terminating with a right angle bend in the probe.

After the core and heat flow were completed we steamed to the northern part of the survey area. From there we ran an airgun sonobuoy line from NNE to SSW down the crest of Ninetyeast Ridge. For this we used the two large airguns with approx. 1600 cubic inches of air for each shot. Clear refractions were observed on the analog records.

A track chart showing the survey lines, the sonobuoy stations and the core is included as figure 1.

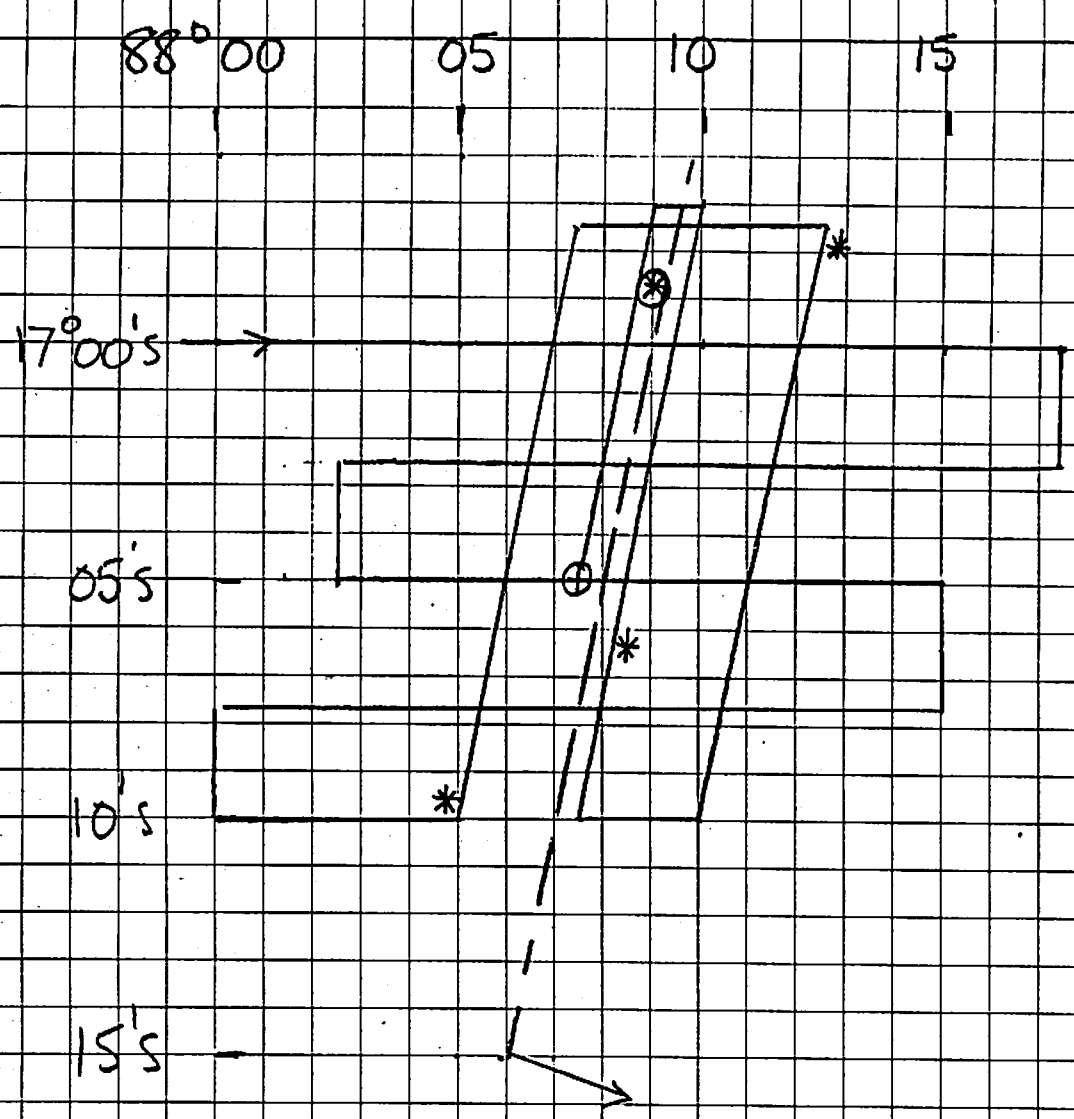

— SCS water gun survey lines.

* water gun sono-buoy.

⊛ airgun sono-buoy.

– – – airgun sono-buoy line.

⊕ core position.